415
902
Digest 6

PWAC-300
DEVELOPMENT OF AIR TURBINE DRIVE COMPONENTS FOR THE PRATT & WHITNEY AIRCRAFT LIQUID METAL TURBOPUMP, TP-1

PRATT & WHITNEY AIRCRAFT
DIVISION OF UNITED AIRCRAFT CORPORATION
CANEL
MIDDLETOWN CONNECTICUT

PWAC-300
DEVELOPMENT OF AIR TURBINE DRIVE COMPONENTS FOR THE PRATT & WHITNEY AIRCRAFT LIQUID METAL TURBOPUMP, TP-1

CONTRACT
AF 33(600)-41233

FORMERLY
NOas 58-662-c

Issued
June 30, 1960

PRATT & WHITNEY AIRCRAFT
DIVISION OF UNITED AIRCRAFT CORPORATION
CANEL
MIDDLETOWN CONNECTICUT

DISTRIBUTION

Category C-85 Standard Distribution List M-3679, 24th Ed.

	Copy No.
Air Force Ballistic Missile Division	1-4
AF Plant Representative, Boeing, Seattle	5-6
AF Plant Representative, Douglas, Long Beach	7
AF Plant Representative, Douglas, Santa Monica	8-10
AF Plant Representative, Lockheed, Marietta	11-14
AF Plant Representative, North American, Downey	15
AF Plant Representative, North American, Los Angeles	16
Air Force Special Weapons Center	17-18
Air Research and Development Command (RDRRA)	19-20
Air Technical Intelligence Center	21
Air University Library	22
ANP Project Office, Convair, Fort Worth	23-25
Albuquerque Operations Office	26
Argonne National Laboratory	27
Army Ballistic Missile Agency	28-29
Army Rocket and Guided Missile Agency	30
Assistant Secretary of Defense, R&D (WSEG)	31
Assistant Secretary of the Air Force, R&D	32
Atomic Energy Commission, Washington	33-38
Atomics International	39
Battelle Memorial Institute	40
Brookhaven National Laboratory	41
Bureau of Naval Weapons	42-43
Bureau of Naval Weapons General Representative	44
BUWEPSREP, Aerojet-General, Azusa	45
BUWEPSREP, Chance Vought, Dallas	46
BUWEPSREP, Convair, San Diego	47
BUWEPSREP, Goodyear Aircraft, Akron	48
BUWEPSREP, Grumman Aircraft, Bethpage	49
BUWEPSREP, Martin, Baltimore	50
Bureau of Ships	51
Bureau of Yards and Docks	52
Chicago Operations Office	53-54
Chicago Patent Group	55
Defense Atomic Support Agency, Washington	56
Director of Naval Intelligence	57
duPont Company, Aiken	58
General Electric Company (ANPD)	59-66
General Electric Company, Richland	67-69
Hartford Aircraft Reactors Area Office	70
Idaho Test Division (LAROO)	71
Jet Propulsion Laboratory	72
Knolls Atomic Power Laboratory	73

	Copy No.
Lockland Aircraft Reactors Operations Office	74
Los Alamos Scientific Laboratory	75-76
Marquardt Aircraft Company	77
National Aeronautics and Space Administration, Cleveland	78
National Aeronautics and Space Administration, Hampton	79
National Aeronautics and Space Administration, Washington	80
Naval Air Development Center	81
Naval Air Material Center	82
Naval Air Turbine Test Station	83
Naval Research Laboratory	84
New York Operations Office	85
Oak Ridge Operations Office	86
Office of Naval Research	87
Office of the Chief of Naval Operations	88
Patent Branch, Washington	89
Phillips Petroleum Company (NRTS)	90-91
Sandia Corporation	92
Sandia Corporation, Livermore	93
School of Aviation Medicine	94-95
Union Carbide Nuclear Company (ORNL)	96-103
USAF Headquarters	104
USAF Project RAND	105-106
U. S. Naval Postgraduate School	107
U. S. Naval Radiological Defense Laboratory	108
University of California, Livermore	109-110
Westinghouse Bettis Atomic Power Laboratory	111-113
Wright Air Development Division	114-126
Technical Information Service Extension	127-151
BUREAU OF NAVAL WEAPONS	
Bureau of Naval Weapons, East Hartford	152-166
PRATT & WHITNEY AIRCRAFT	
CANEL	167-181

TABLE OF CONTENTS

	Page No.
Table of Figures	5
I. Summary	7
II. Introduction	11
III. Aerodynamic Tests of Turbine Inlet Scroll Models	15
A. Background and Purpose	17
B. Description of Model Test Scrolls	18
C. Test Equipment and Facilities	33
D. Instrumentation	35
E. Test Procedure	37
1. RS-7 Model Scroll Tests	37
2. Tangential Scroll Model Tests (RS-11 through RS-15)	37
F. Results of Tests	38
1. Head Loss Coefficients	38
2. Circumferential Velocity Distribution	38
G. Discussion of Results	42
H. Conclusions	43
IV. Structural Tests of the Prototype Turbine Inlet Scroll	45
A. Background and Purpose	47
B. Description of Prototype Test Scroll	47
C. Test Equipment and Instrumentation	47
D. Test Procedure	50
E. Results of Tests	50
F. Discussion of Results	56
V. Turbine Face Seal Development	57
A. Background and Purpose	59

	Page No.
B. Description of Test Face Seals	59
C. Description of Test Equipment and Instrumentation	59
D. Test Procedure	67
E. Discussion of Results	68
VI. Appendix	71
A. Data Reduction Equations	73

TABLE OF FIGURES

Figure No.	Title	Page No.
1	Original Scroll Model RS-7 Installed in Test Stand	19
2	Turbine Inlet Model RS-7 with Modifications	20
3	Drawings of RS-7 Model Turbine Inlet Scroll	21
4	Illustration Showing Area Ratio of Inlet Support Vanes	23
5	Prototype Stainless Steel TP-1 Turbine Inlet Scroll	24
5	Tangential Inlet Turbine Scroll Models	25
7	Drawing of Model RS-11 Turbine Inlet Scroll	26
8	Drawing of Model RS-12 Turbine Inlet Scroll	27
9	Drawing of Model RS-13 Turbine Inlet Scroll	28
10	Drawing of Model RS-14 Turbine Inlet Scroll	29
11	Drawing of Model RS-15 Turbine Inlet Scroll	30
12	Turbine Inlet Model Scroll with Instrumented Exit Adapter Assembly	31
13	Exit Adapter with Turning Vanes Installed	32
14	Model Turbine Inlet Scroll Test Stand	34
15	Instrumentation Schematic of Air Scroll Test Stand	36
16	Table of Head Loss Coefficients and Velocity Distributions for All Models Tested	39
17	Circumferential Velocity Distribution for All Modifications of the Model RS-7 Scroll	40
18	Circumferential Velocity Distribution for the Tangential Inlet Model Scrolls	41
19	Prototype Stainless Steel TP-1 Turbine Air Inlet Scroll on the Hydrostatic Structural Test Stand	48
20	TP-1 Air Inlet Scroll Pressure Control Schematic	49

Figure No.	Title	Page No.
21	Stresscoat Crack Pattern at 175 Positive Pressure in the Vicinity of the Inlet Duct	51
22	Stresscoat Crack Pattern at 175 psi Positive Pressure Along Circumferential Weld	52
23	Stresscoat Crack Pattern at 175 psi Negative Pressure in the Vicinity of the Outer Radius of the Welds	53
24	Stresscoat Crack Pattern at 175 psi Negative Pressure at the Inner Radius of the Vane Welds	54
25	Table of Hydrostatic Stress Test Results of TP-1 Turbine Inlet Scroll	55
26	Schematic of Turbine Face Seal and Labyrinth	60
27	Test Rig Installation Schematics of Commercial Turbine Face Seals	61
28	Sealol Face Seal after 208 Hours of Testing	62
29	Chicago Rawhide Seal after 34 Hours of Testing	63
30	Cartriseal Seal after 282 Hours of Testing	64
31	Test Stand Used for Turbine Face Seal Evaluation	65
32	Schematic of Oil Leakage Measuring Device	66
33	Tabulated Summary of the TP-1 Turbine Face Seal Test Results	69

I. SUMMARY

DEVELOPMENT OF AIR TURBINE DRIVE COMPONENTS FOR THE PRATT & WHITNEY AIRCRAFT LIQUID METAL TURBOPUMP, TP-1

Written By: J. S. MURPHY
R. S. LOMBARD
R. G. HASKELL
J. D. SUTHERLAND

Checked By: G. M. Wood
G. M. Wood
Assistant Project Engineer

Approved By: R. W. Kelly
R. W. Kelly
Project Engineer

UNCLASSIFIED
CLASSIFICATION

R. W. Kelly
AUTHORIZED CLASSIFIER

June 30, 1960
DATE

I. SUMMARY

This report has been prepared in accordance with the requirements of Air Force Contract AF33(600)-41233, formerly Department of the Navy, Bureau of Aeronautics Contract Noas 58-662-c, Item 18 of Lot II.

The components testing program for development of the TP-1 air turbine drive consisted of a) full scale fiberglass model tests of the TP-1 turbine inlet scroll using subsonic air, b) subsonic air tests of five tangential inlet type fiberglass turbine inlet scroll models, c) cold hydrostatic tests of the prototype TP-1 turbine scroll using a stresscoat technique, d) evaluation tests of three types of carbon face seals, and e) a single endurance test of the most promising carbon face seal. As a result of these component development tests, satisfactory modifications to the prototype turbine inlet scroll were effected, the operating stress levels in the scroll at design conditions were determined to be non-critical, and the performance of the best carbon face seal tested was found to be acceptable from a leakage standpoint. A successful endurance test of approximately 1400 hours was conducted on this seal with an average leakage of about 0.5 cc/hr.

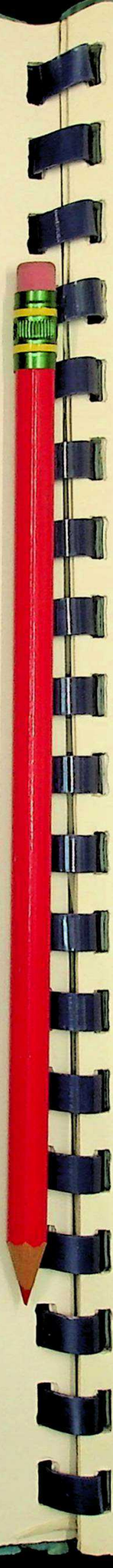

II. INTRODUCTION

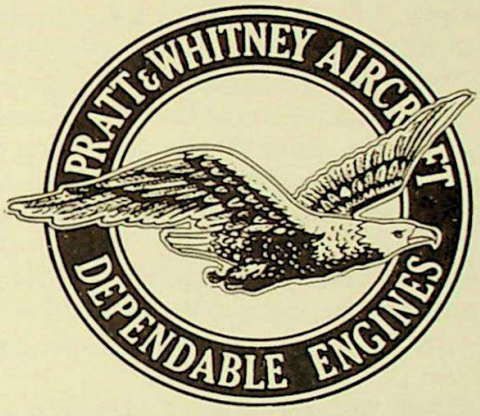

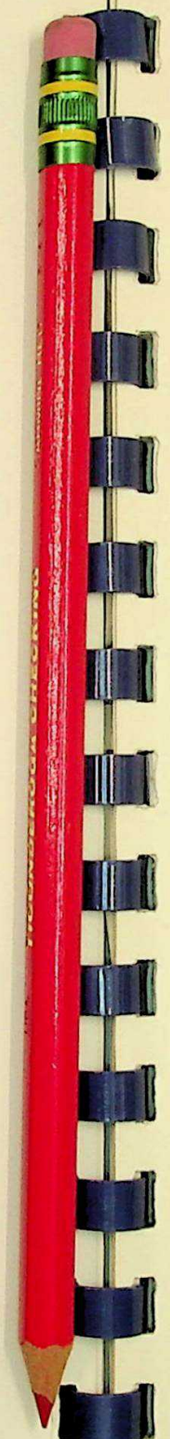

II. INTRODUCTION

The development of a 1425F air turbine drive for the liquid metal turbopump required detailed testing of such vital components as the turbine inlet scroll and the turbine face seal. This turbopump was designed as a directly coupled unit to pump 3000 gpm of 1300F NaK with a developed head rise of 400 feet at a speed of 8000 rpm. To obtain the highest aerodynamic efficiency of the turbine, the inlet scroll must distribute the air flow uniformly circumferentially to the nozzle assembly with a minimum loss of total pressure. Due to the combined pressure and high temperature requirements, a total of sixteen support vanes were incorporated upstream of the turbine nozzle vanes to tie the scroll structure together. Since it is not possible to accurately stress analyze a structure of this configuration, an experimental stresscoat technique was used. Such an investigation is limited to a study of the elastic stress distribution only and does not predict high temperature creep characteristics. However, much very useful information regarding the general stress distribution can be readily obtained by this experimental method. The turbine face seal in a liquid metal turbopump must seal the inert gas blanketed oil system in the bearing compartment from the hot turbine air stream with a minimum loss of the inert gas and oil. To alleviate the operating conditions, a pressure differential of only four psi was imposed across the seal faces by introducing a second source of cool air between the face seal and a labyrinth shaft seal. The test conditions of pressure differential, oil temperature and speed were imposed on various component test seals to evaluate their performance for this application on two available test stands at CANEL.

The aerodynamic scroll tests were conducted on one full scale fiberglass model of the TP-1 design plus five other available fiberglass models which were designed with tangential type inlets. All scrolls were tested on the existing subsonic air test stand at CANEL.

Three other reports which are directly related to this phase of the TP-1 turbopump development program are:

1. PWAC-297 - "Pump Tests Conducted for the Development of the Pratt & Whitney Aircraft Liquid Metal Turbopump, TP-1".

2. PWAC-298 - "Development of Pump Components for the Pratt & Whitney Aircraft Liquid Metal Turbopump, TP-1".

3. PWAC-299 - "Performance Tests of the Air Turbine for the Pratt & Whitney Aircraft Liquid Metal Turbopump, TP-1".

This report includes in, the order mentioned, descriptions of the turbine inlet model scroll experiments, hydrostatic stresscoat tests of the prototype inlet scroll, and evaluation tests of three types of turbine carbon face seals including one endurance test.

TICONDEROGA CHECKING

III. AERODYNAMIC TESTS OF TURBINE INLET SCROLL MODELS

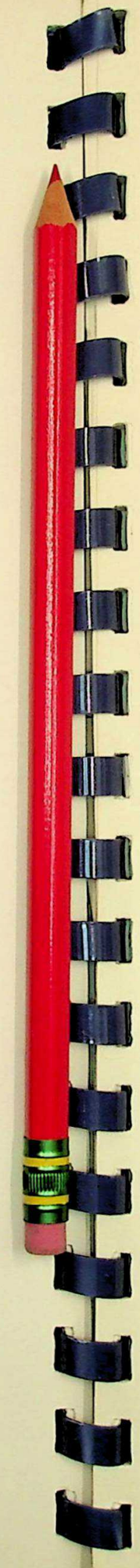

A. BACKGROUND AND PURPOSE

The purpose of this test program was to evaluate scrolls of various geometries to enable selection of an optimum design for directing air to the TP-1 turbopump. A toroidial shaped scroll with a radial inlet, designated as the RS-7 model, was constructed to full scale in fiberglass to expedite testing. The original scroll configuration was modified during development in order to improve its aerodynamic performance characteristics. A more rapid development of this scroll configuration was possible due to the experience gained from the experimental program of the scrolls reported on previously in PWAC-267.

Tests were also conducted on five additional fiberglass scroll models, designated RS-11, RS-12, RS-13, RS-14, and RS-15 which were available for this program. The scroll body configurations of these scrolls were all different and they were all designed with tangential type inlet ducts. This portion of the test program was limited to preliminary evaluation only. The various scrolls were evaluated on the basis of 1) the circumferential midstream velocity distribution in the exit annulus and 2) the total pressure loss through the scrolls.

The report includes, in the order mentioned, descriptions of the models tested, test equipment and facilities, test procedure, and test results. This is followed by a discussion of the results and the appendix.

B. DESCRIPTION OF MODEL TEST SCROLLS

Two basic forms of turbine inlet scrolls were tested; the radial inlet type and the tangential inlet type.

The Radial Inlet Model Scroll

The radial inlet types of model scrolls tested included the RS-7, RS-7 Modification I, and the RS-7 Modification II.

The RS-7 Model - Original Configuration

The original test unit is shown in the test stand in Fig 1. The inlet shown in Fig 2 was a five inch cylinder with its axis in the axial plane at an angle of 120 degrees to the exit annulus. A sectional view of this scroll model is shown in Fig 3. Sixteen vanes were utilized for structural support near the point of fluid discharge from the scroll into the exit annulus. Tests were run with varying numbers of these vanes in order to determine their effect on performance.

Upon receipt of the prototype stainless steel nozzle ring, it was placed downstream of the pressure taps in the exit annulus and the unit was tested to get an indication of its effect on the aerodynamic performance of the model scroll.

Model RS-7 Modification I

The first modification of the inlet ducting to the RS-7 model scroll was made in an attempt to improve its performance characteristics and is shown in Figs 2 and 3. This change consisted of positioning the five inch diameter inlet duct perpendicular to the scroll body axis. During the tests with this inlet, the original inlet was plugged with a wooden block shaped to fit the contour of the scroll body.

Test runs were made using various combinations of the scroll support vanes mentioned previously and also with the prototype turbine nozzle vane assembly installed.

Model RS-7 Modification II

The model RS-7 Modification II, shown in Figs 2 and 3, was the second inlet ducting revision to the original test unit. This inlet was also positioned perpendicular to the scroll axis and was shaped as a constant area transition from a circular duct to a nearby elliptical cross section at the junction with the scroll body. Both of the previously tested inlets were plugged with wooden blocks shaped to the contour of the scroll body. A flow splitter was inserted in the middle of the inlet section to maintain steady flow conditions with this particular configuration. For this series of tests, the scroll was tested only with the full complement of 16 support vanes. It was also run with and without the prototype nozzle ring in position.

For structural design reasons, it became necessary to add two support vanes, or several support dowels, in addition to the flow splitter in the inlet duct section. Test runs were made with wooden dowels in the inlet transition duct to determine their effect on performance. Several other runs were made with dowels wrapped in shim stock to simulate vanes.

ORIGINAL SCROLL MODEL RS-7 INSTALLED IN TEST STAND

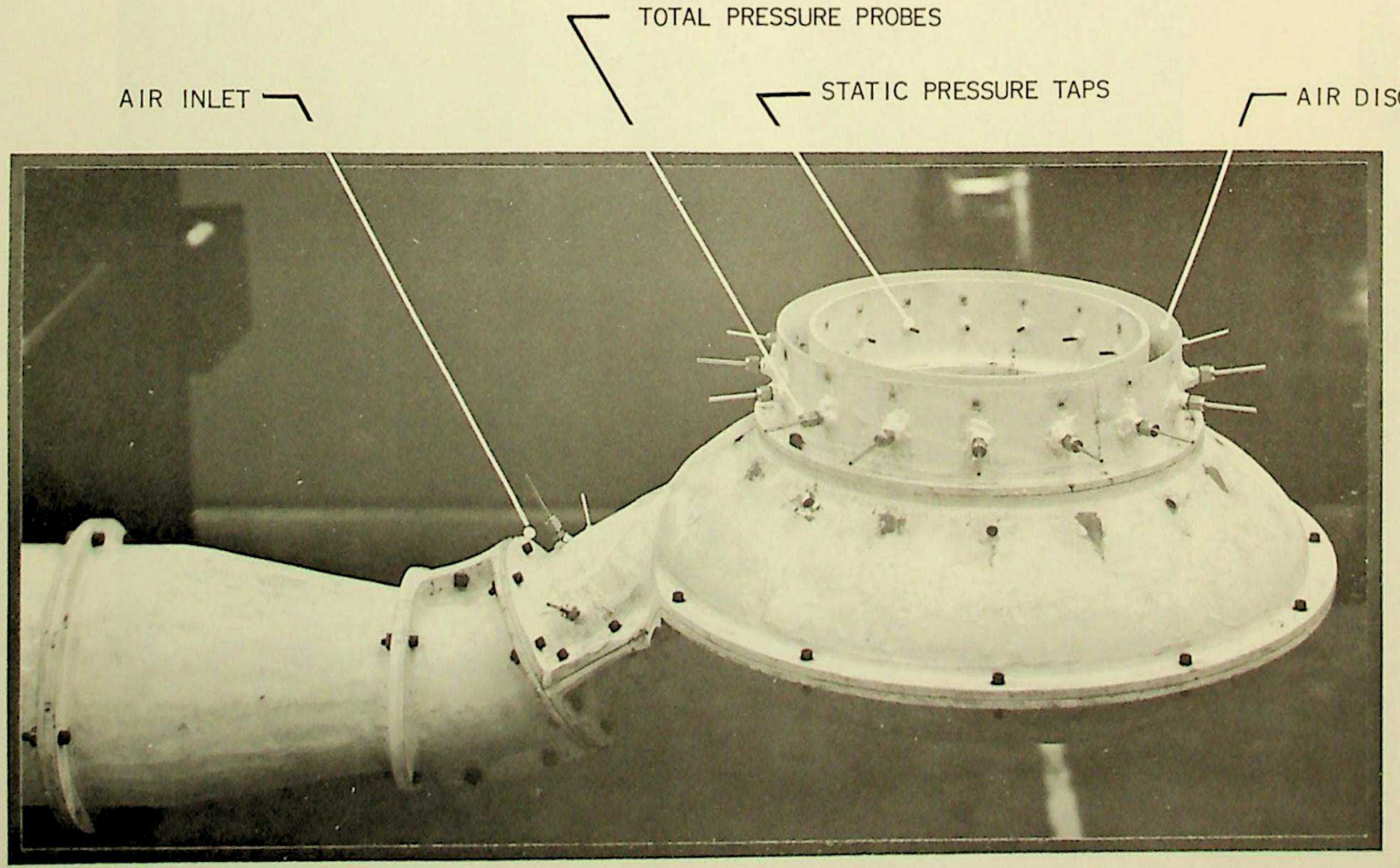

PWAC - 300
FIG 1

8D5190

TURBINE INLET SCROLL MODEL RS-7 WITH MODIFICATIONS

SHOWING THREE INLETS

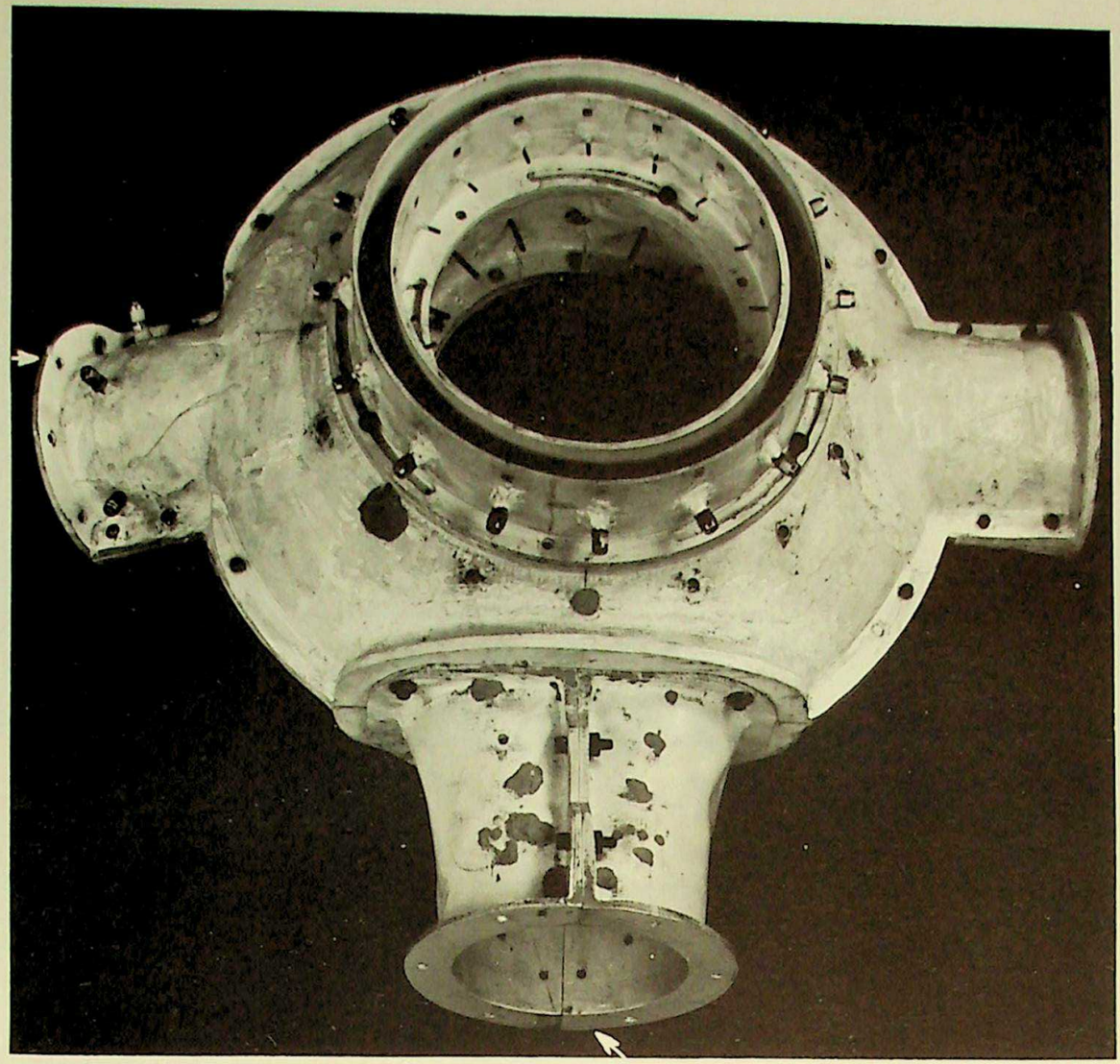

PWAC- 300

FIG 2

TIDEWATER CRAFTING CARMINE RED

FIG 3

DRAWINGS OF RS7 MODEL TURBINE INLET SCROLL

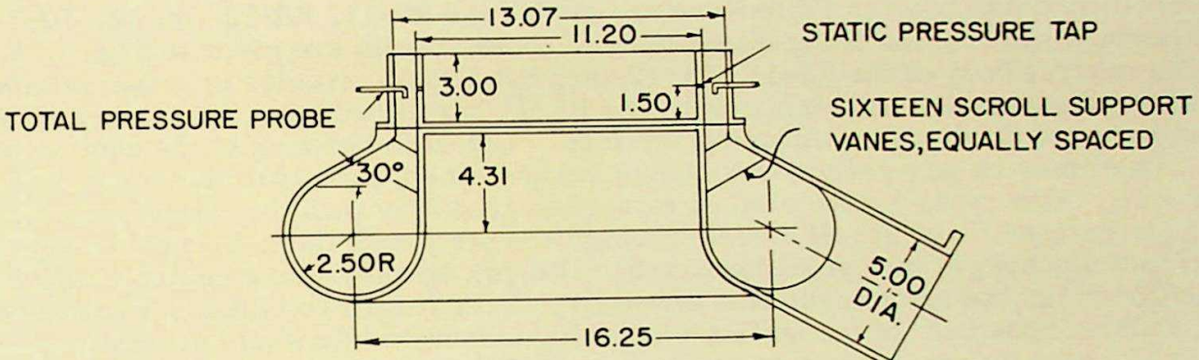

A ORIGINAL CONFIGURATION

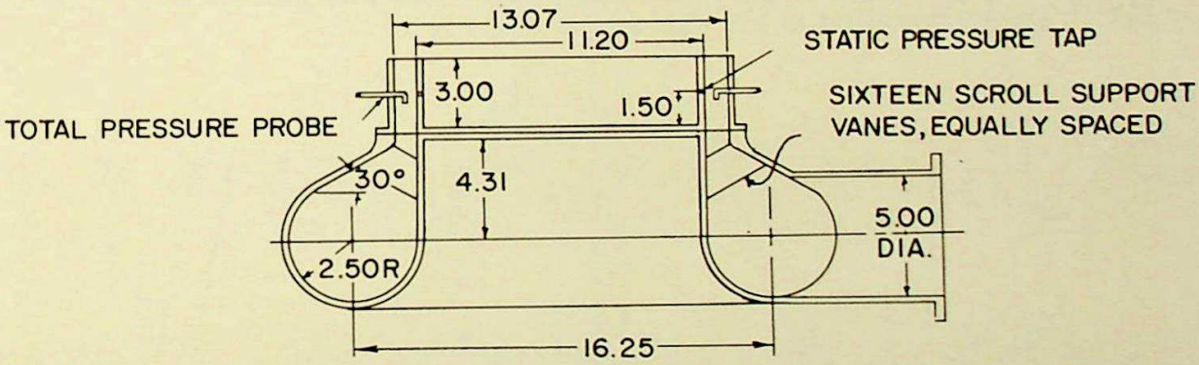

B MODIFICATION I

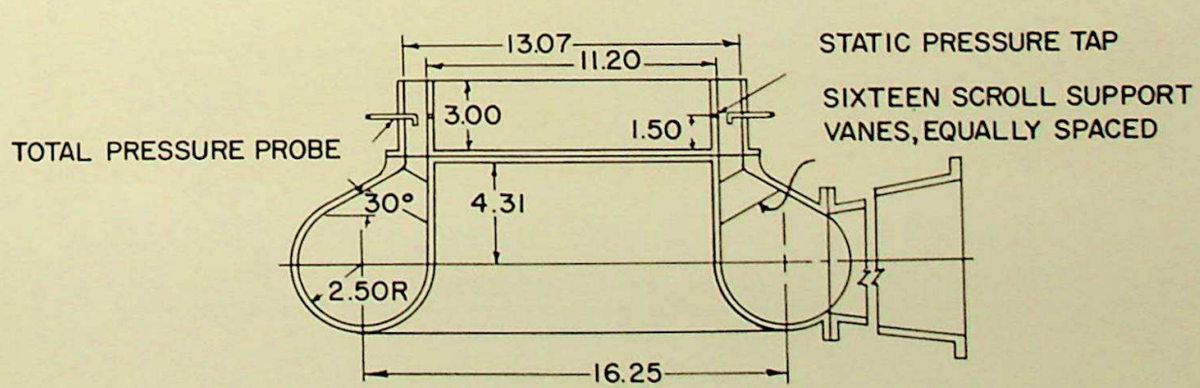

C MODIFICATION II

These simulated vane tests were arranged so as to vary the cross sectional area between the vanes at the leading edges to the cross sectional area between them at the trailing edges as illustrated in Fig 4. In effect, these area ratios governed the amount of acceleration or deceleration of the flow through each of the four flow paths in the inlet duct section. Tests were run at area ratios of 1.26, 1.07, 0.85, 0.65, 0.51, and 0.43. The prototype turbine inlet scroll fabricated from type 316 stainless steel with an area ratio of 0.90 is shown in Fig 5.

The Tangential Inlet Type Scroll Models

The five scroll models shown in Fig 6 were designated the RS-11, RS-12, RS-13, RS-14, and RS-15. Drawings showing the basic dimensions of these scrolls are given in Figs 7, 8, 9, 10, and 11. The central body of the RS-11, RS-12, and RS-13 was circular in cross section and of gradually changing area circumferentially. The RS-14 scroll body was square in cross section and of constant area at all circumferential stations. The cross section of the central body of the RS-15 model may be generally described as being formed of conical side walls with an elliptical outer wall. The cross sectional area increased gradually with the circumferential flow path. The air entered these scroll models through the tangential inlet, passed through the scroll body and discharged into an exit adapter. The exit adapter was common to all these scrolls and contained the instrumentation necessary to record the total and static pressure in the exit annulus upstream of the station where the turbine nozzle would normally be located. The adapter is shown in cross section mounted on the RS-11 model scroll in the drawing of Fig 7 and mounted on the RS-15 scroll in the photograph shown in Fig 12.

The initial testing of the scroll indicated that the exit flow contained large tangential or swirl velocity components. To reduce this swirl a turning vane assembly consisting of eight vanes to turn the flow to about 30 degrees from the tangential plane was fabricated. This turning vane assembly is shown installed in the exit adapter in Fig 13.

FIG 4

LUSTRATION SHOWING AREA RATIO OF INLET SUPPORT VANES

SCROLL MODEL RS-7 MODIFICATION II

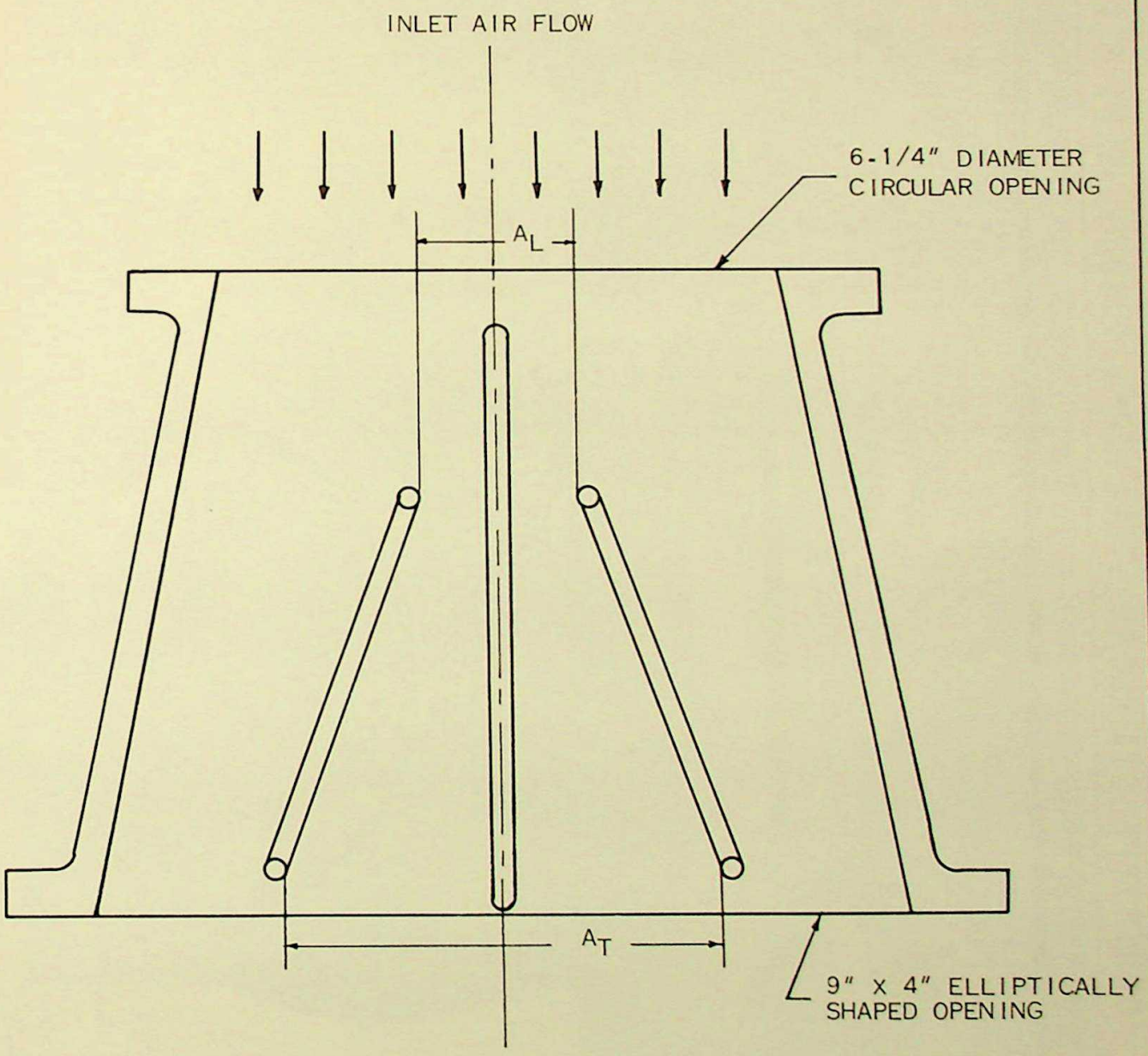

$$\text{AREA RATIO} = \frac{\text{CROSS SECTIONAL AREA OF FLOW PATH AT } A_L}{\text{CROSS SECTIONAL AREA OF FLOW PATH AT } A_T}$$

PROTOTYPE STAINLESS STEEL TP-1 TURBINE INLET SCROLL

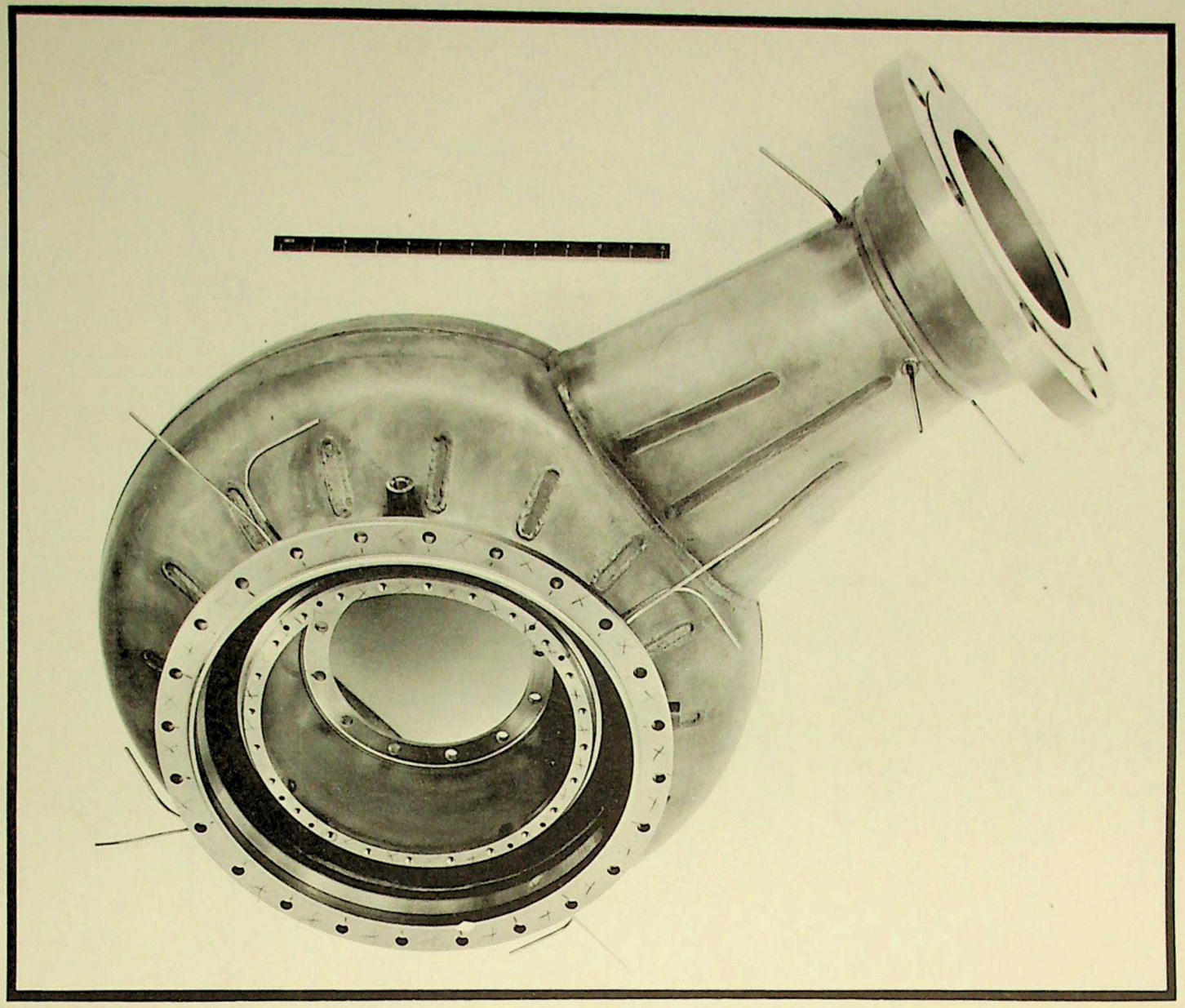

PWAC - 300
FIG 5

TANGENTIAL INLET TURBINE SCROLL MODELS

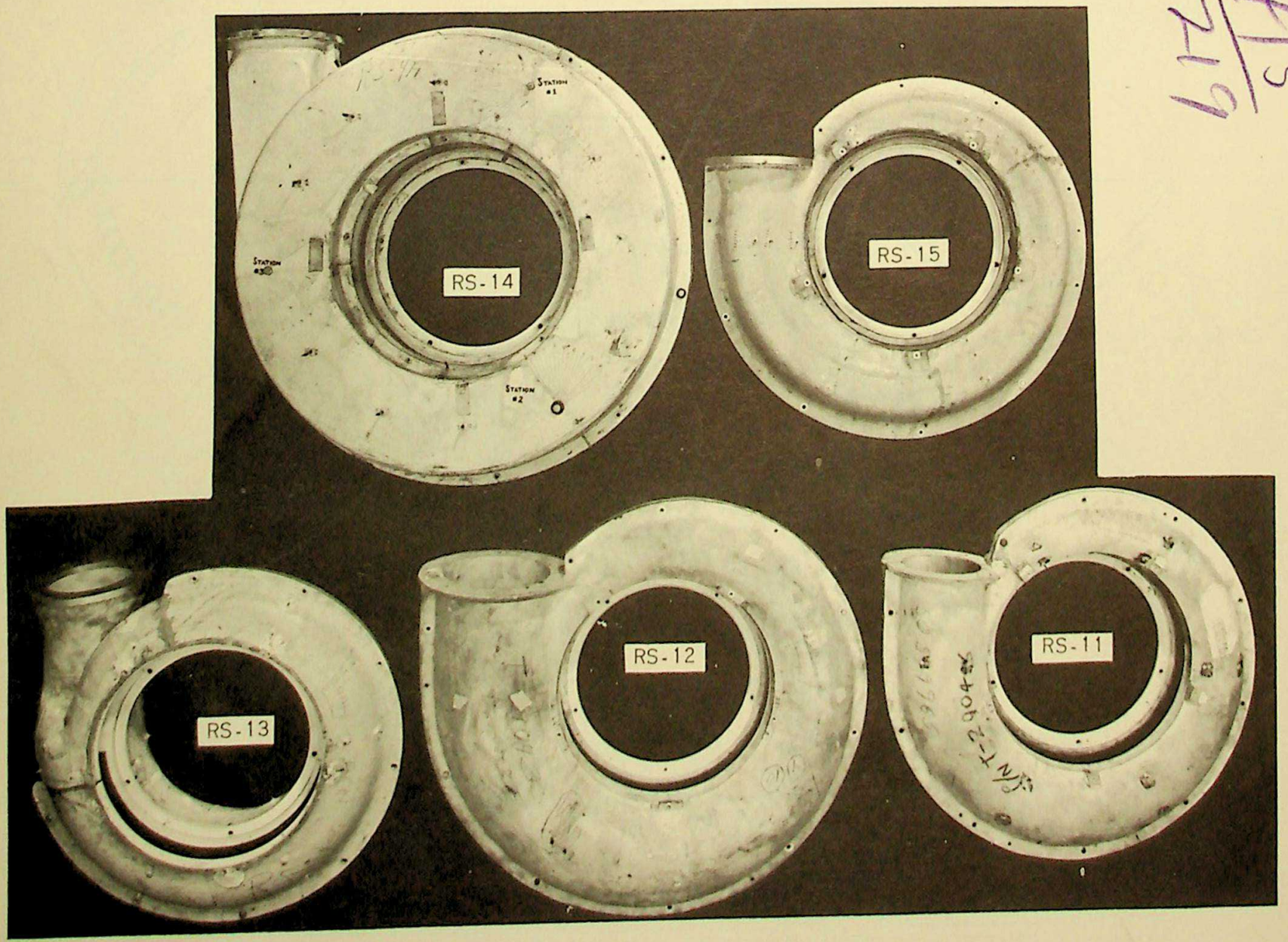

PWAC - 300
FIG 6

DRAWING OF MODEL RS-11 TURBINE INLET SCROLL

WITH EXIT ADAPTER

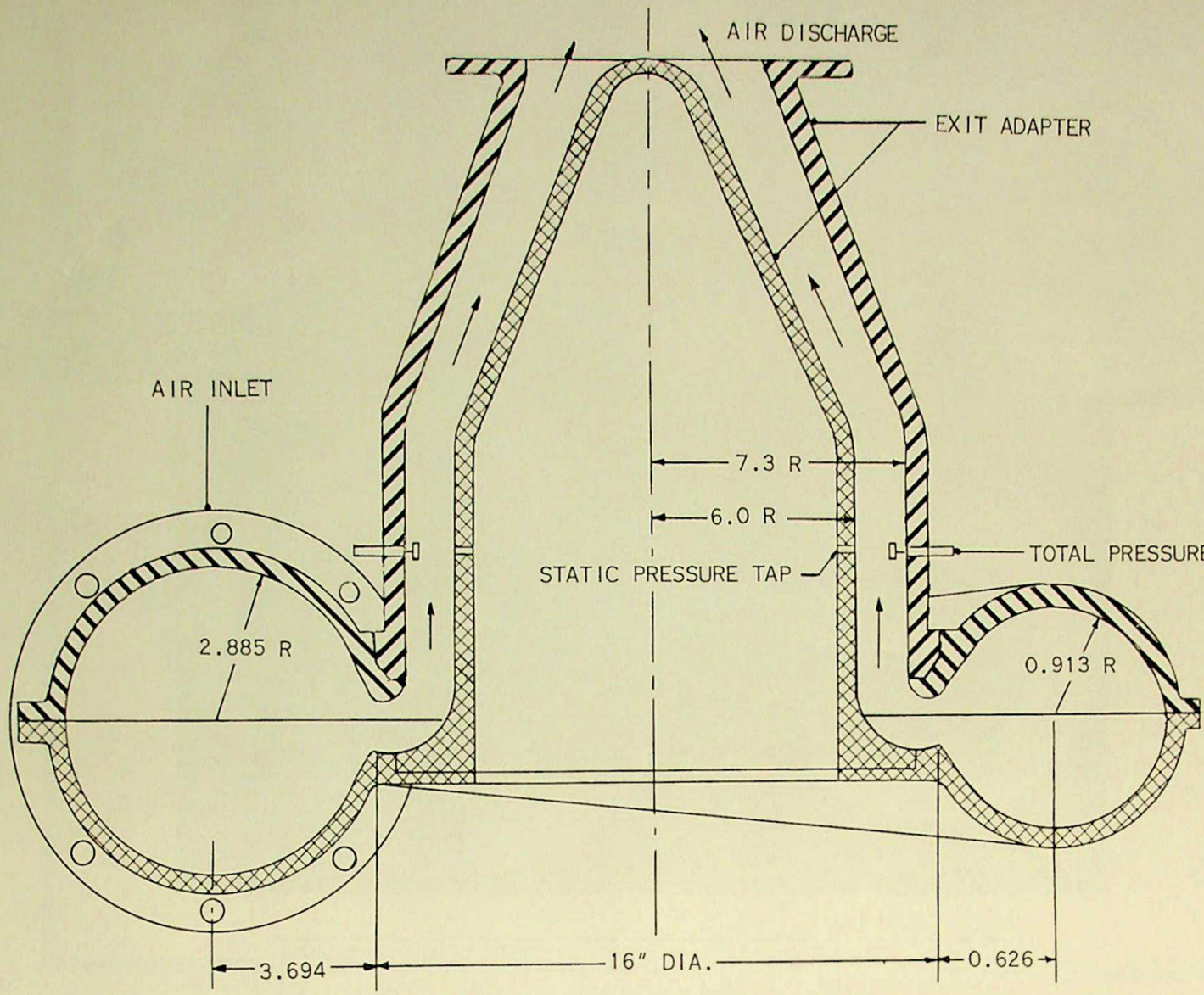

PWAC- 300
FIG 7

FIG 8

DRAWING OF MODEL RS-12

TURBINE INLET SCROLL

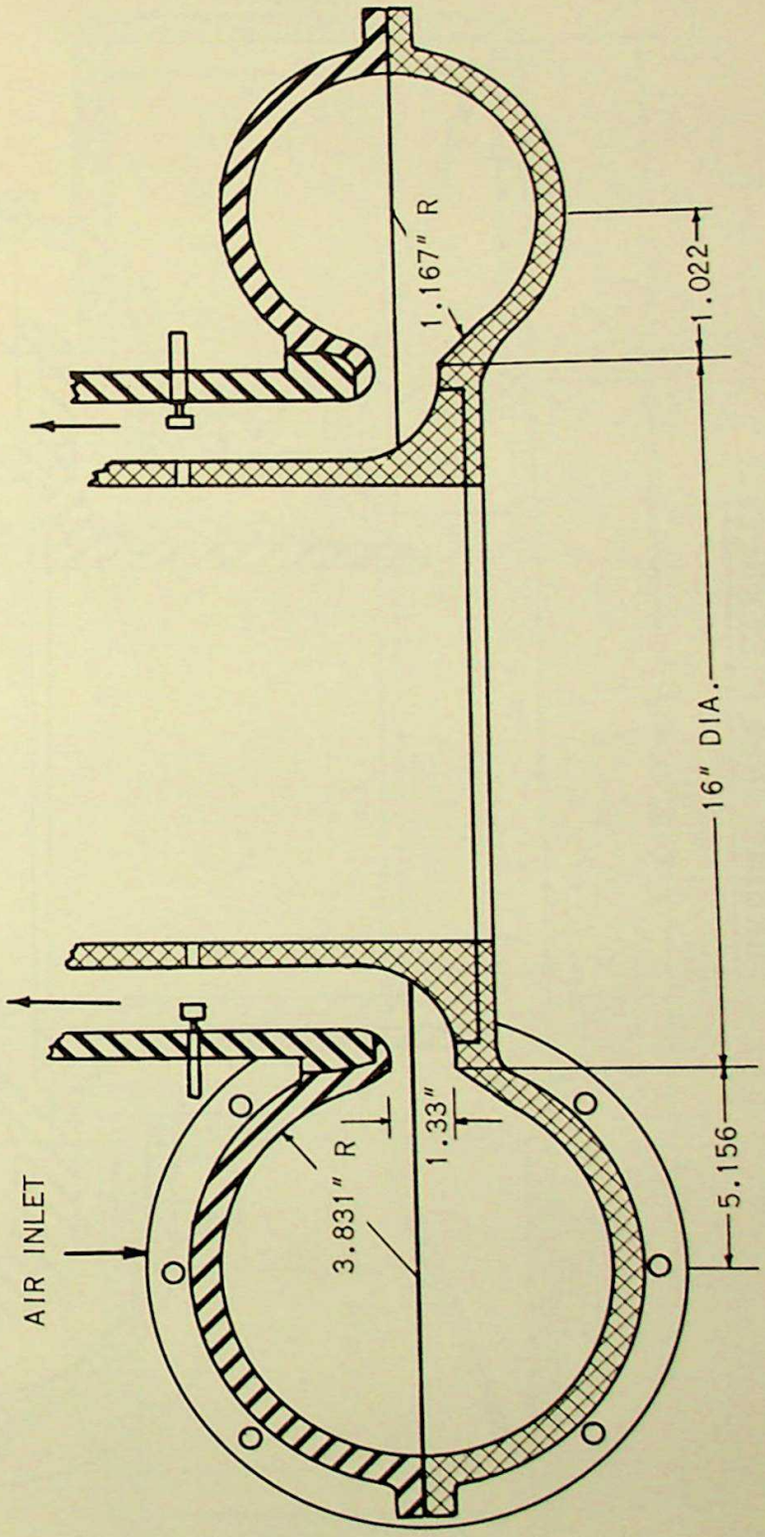

DRAWING OF MODEL RS-13
TURBINE INLET SCROLL

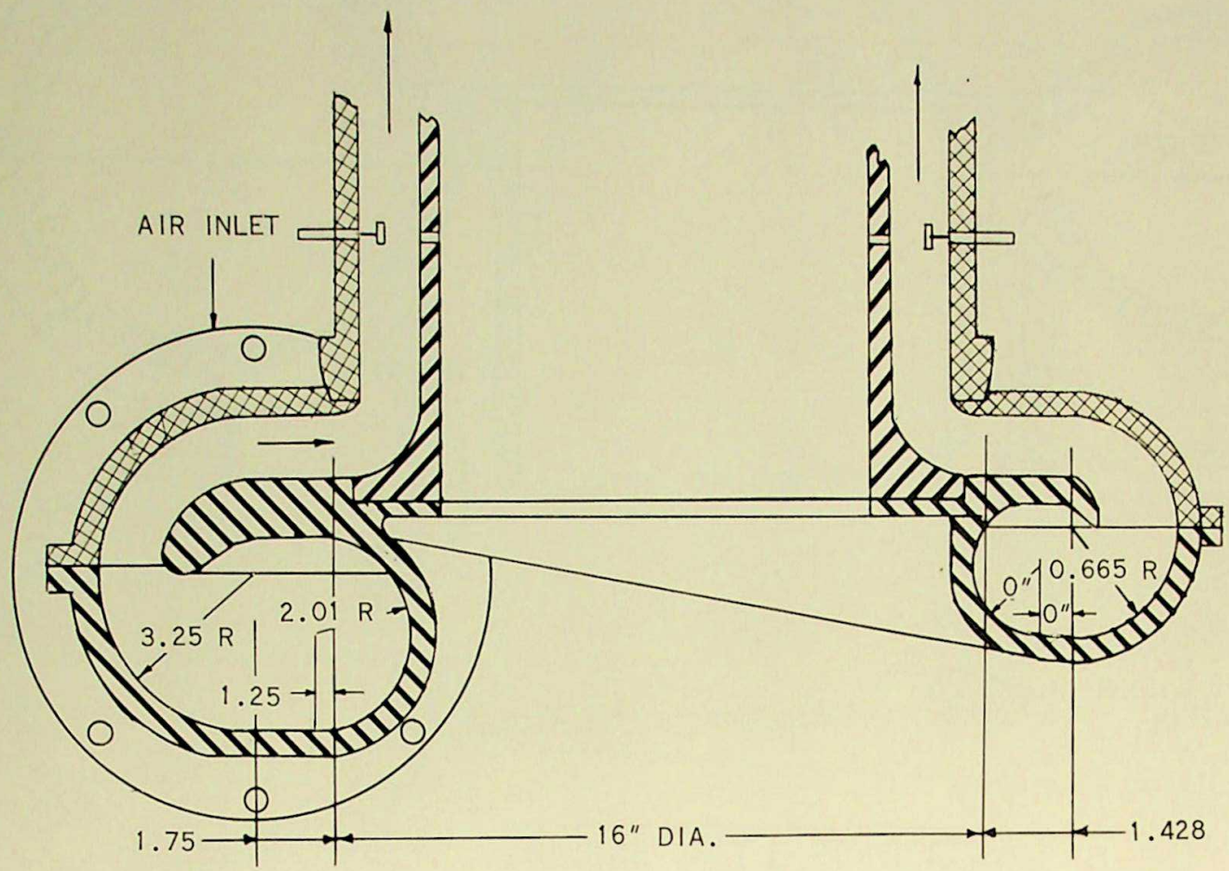

PWAC - 300
FIG 9

FIG 10

DRAWING OF MODEL RS-14

TURBINE INLET SCROLL

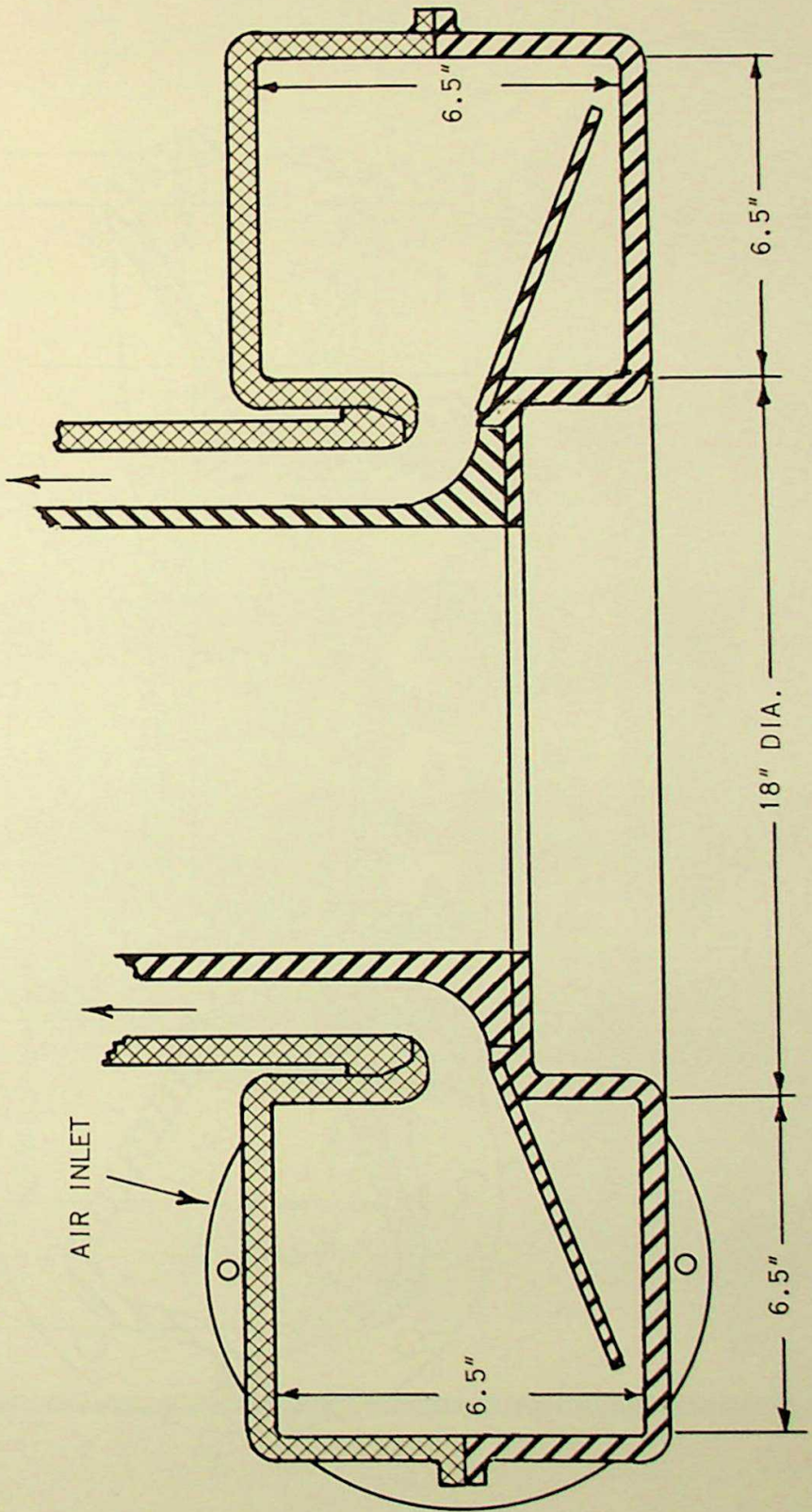

DRAWING OF MODEL RS-15

TURBINE INLET SCROLL

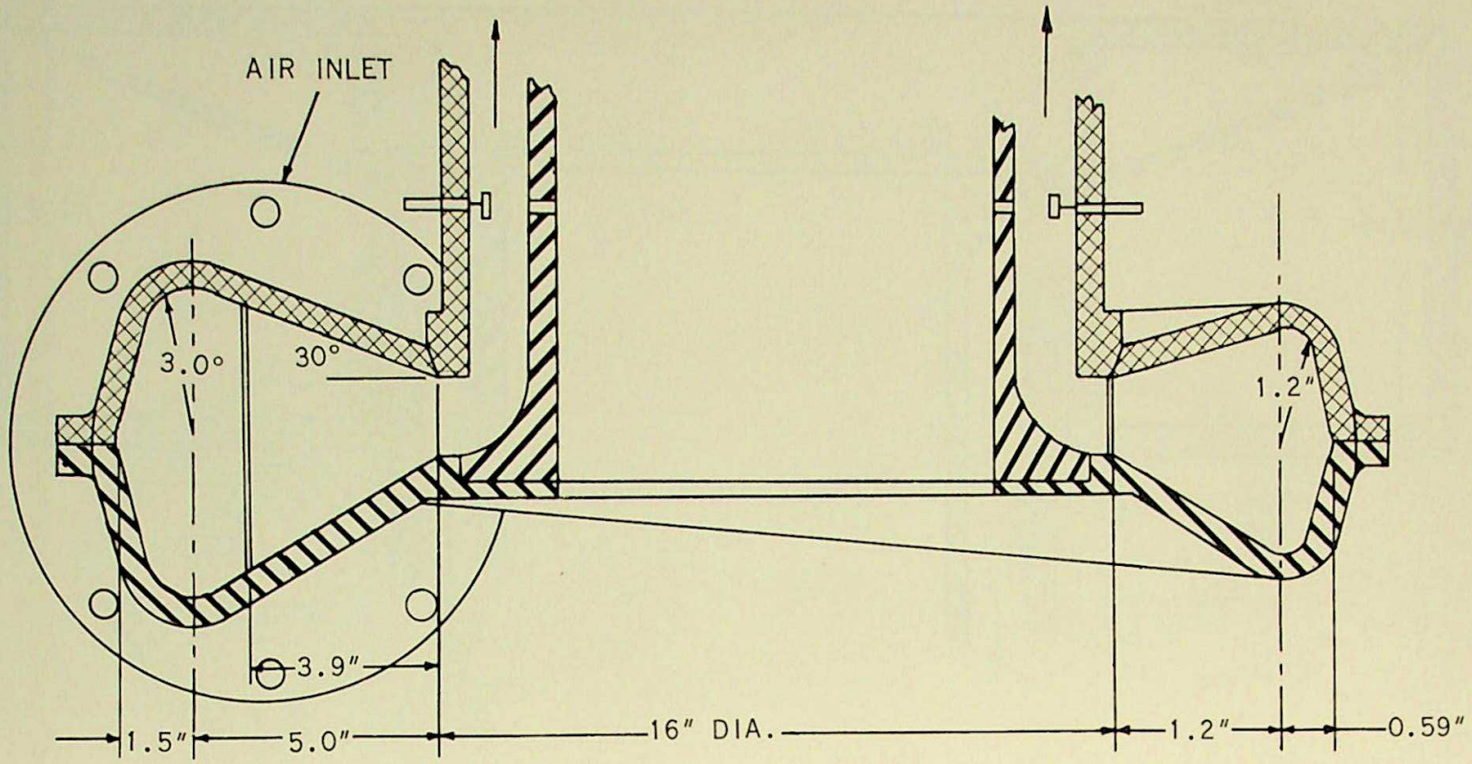

PWAC - 300
FIG 11

FIG 12

TURBINE INLET MODEL SCROLL WITH INSTRUMENTED EXIT ADAPTER ASSEMBLY

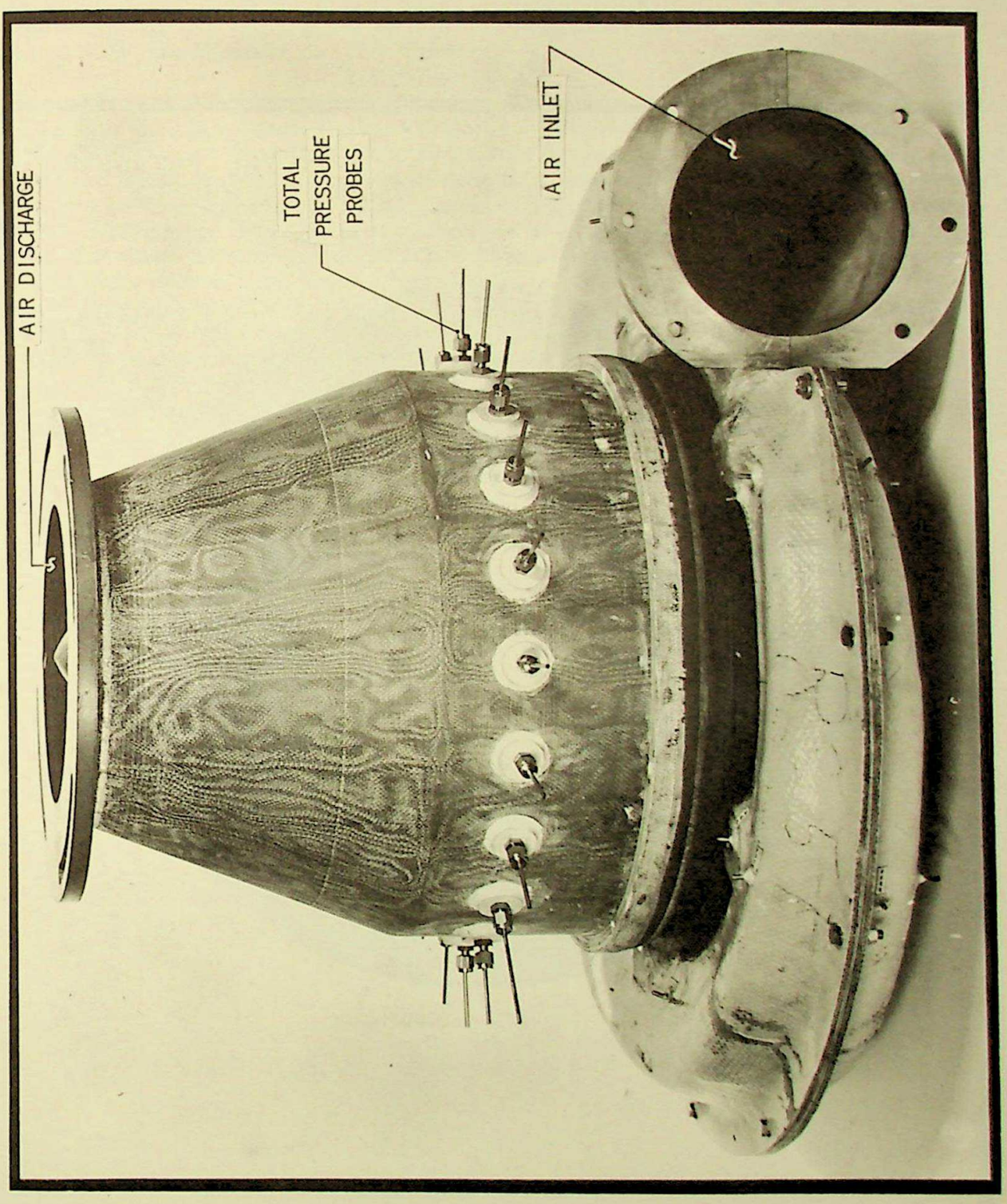

FIG 13

EXIT ADAPTER WITH TURNING VANES INSTALLED

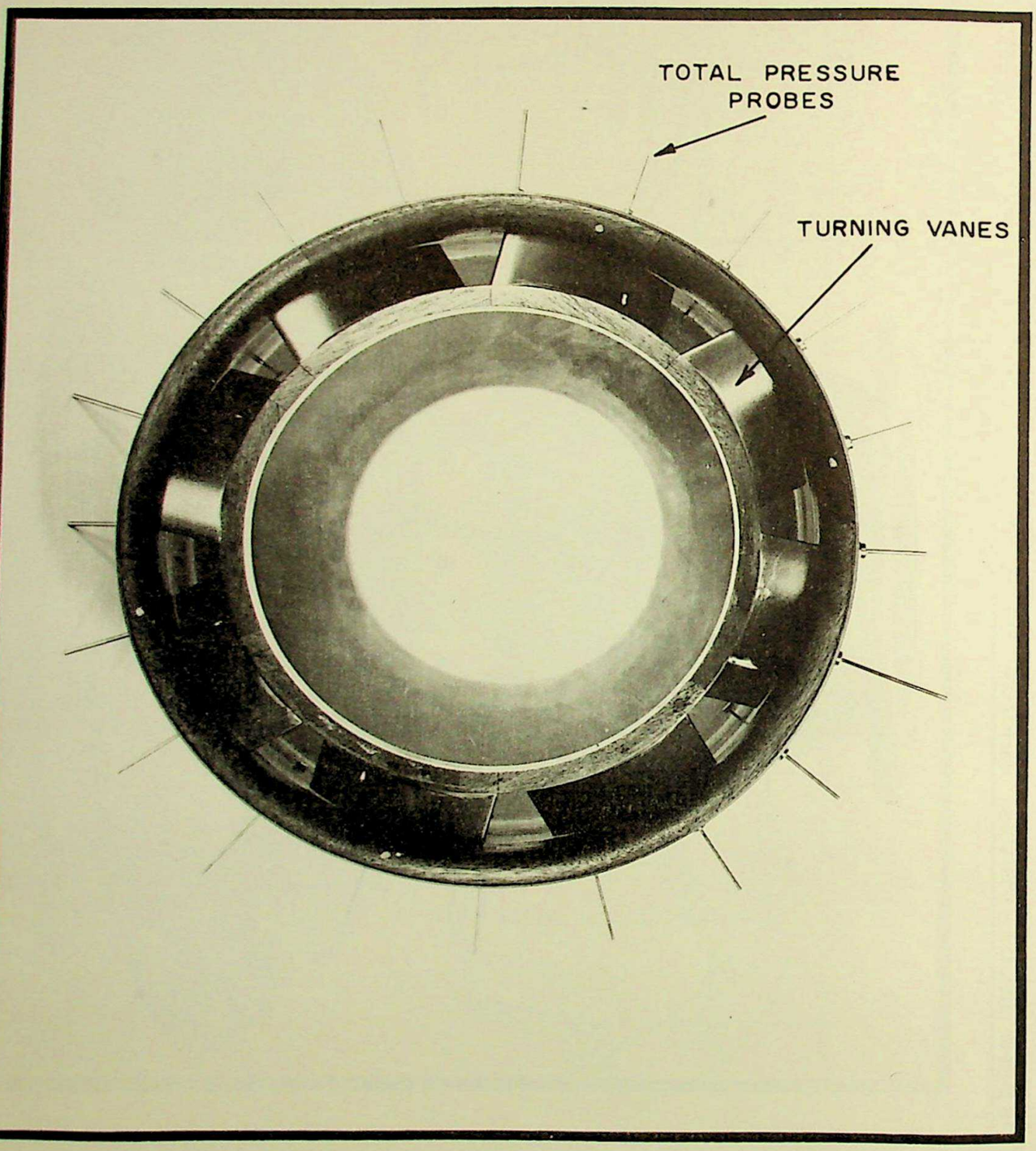

C. TEST EQUIPMENT AND FACILITIES

An over-all photographic view of the test stand is shown in Fig 14. The stand had been operated for approximately two years prior to this test program and was, therefore, completely calibrated and fully operational.

Subsonic air for the test scrolls was supplied by a constant speed, single stage, centrifugal blower driven by a fifty horsepower electric motor. The blower unit was installed in a soundproof plenum chamber and the intake air stream was passed through filtering units. Coarse adjustments were made to the flow rate by means of a butterfly valve in the blower inlet while fine adjustments were accomplished by manual operation of a shutter-type valve in the 16 inch diameter blower discharge duct. A heat exchanger was incorporated downstream of the shutter valve which maintained the air stream at approximately room temperature during the scroll tests. Seven layers of fine wire mesh screening were placed upstream of the flow metering station to provide uniform velocity profile with negligible swirl. An ASME long radius type of flow metering nozzle was incorporated which accelerated the flow from the 16 inch blower discharge duct to an eight inch diameter fiberglass duct. This duct, which was 40 inches long, was equipped with a mounting flange for mounting the various scroll inlets or inlet adapter sections. After passing through the test scroll, the air was either discharged into an eight inch diameter vertical stack which exhausted to the outside atmosphere or discharged inside the laboratory.

MODEL TURBINE INLET SCROLL TEST STAND

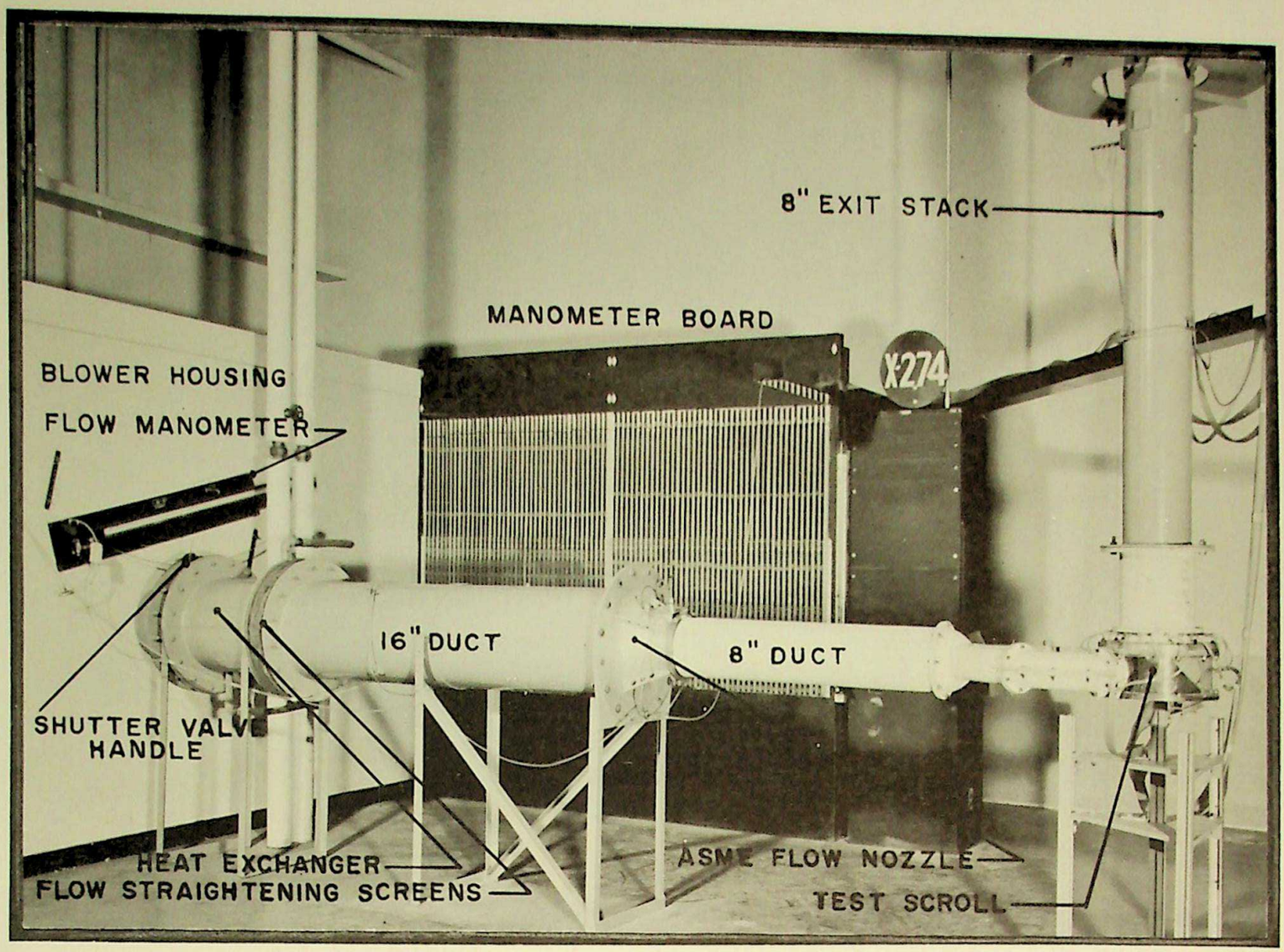

PWAC - 300
FIG 14

D. INSTRUMENTATION

A schematic of the instrumentation used for the turbine model scroll tests is shown in Fig 15.

The nomenclature employed in recording and reducing the experimental pressure and temperature data was as follows:

Symbol	Description and Location
P_{SO}	Average wall static pressure upstream of ASME flow nozzle
P_{S1}	Average wall static pressure at discharge of ASME flow nozzle
P_{V1}	Dynamic pressure at discharge of ASME flow nozzle
P_{T1}	Total pressure at discharge of ASME flow nozzle
P_{S2}	Static pressure at scroll inner wall in the exit annulus
P_{V2}	Dynamic pressure at midstream in scroll exit annulus
P_{T2}	Total pressure at midstream in scroll exit annulus
P_{S3}	Average wall static pressure in the exit stack
P_{T3}	Average total pressure in the exit stack
T_1	Temperature of air measured upstream of ASME flow nozzle

All of the pressures, except the pressure differential across the flow nozzle, were manually recorded on an open type, vertical water manometer board referenced to atmospheric pressure. The ASME flow nozzle differential pressure was read on an inclined water manometer. All pressure data were recorded in inches of water and the air temperature was recorded in degrees Fahrenheit.

The test scrolls were fitted with instrumented sections of the exit annulus to record the midstream total pressure and the inner wall static pressure. The outer instrument ring for the RS-7 model scroll had 16 total pressure probes while the adapter section for the tangential inlet scrolls had 20 total pressure probes. The inner instrumentation ring for the RS-7 model had 16 static pressure taps and the adapter section for the tangential inlet scrolls had 40 static pressure taps.

The instrument rings on the RS-7 model scroll tests had slotted mounting holes which made it possible to rotate the rings through an arc of 45 degrees. An index system was used to position the rings and thus record many more points circumferentially than was possible with 16 fixed stations. This system also afforded the flexibility of placing more than one Kiel probe or static tap at any given circumferential position to cross check the instrumentation. The exit stack was fitted with a manifolded wall static tap station approximately four feet above the test scroll discharge to measure the average static pressure. Two total pressure rakes were mounted across the stack discharge at right angles to each other to record the average total pressure. The exit stack was used on all scroll model testing except the RS-7 model.

INSTRUMENTATION SCHEMATIC OF AIR SCROLL TEST STAND

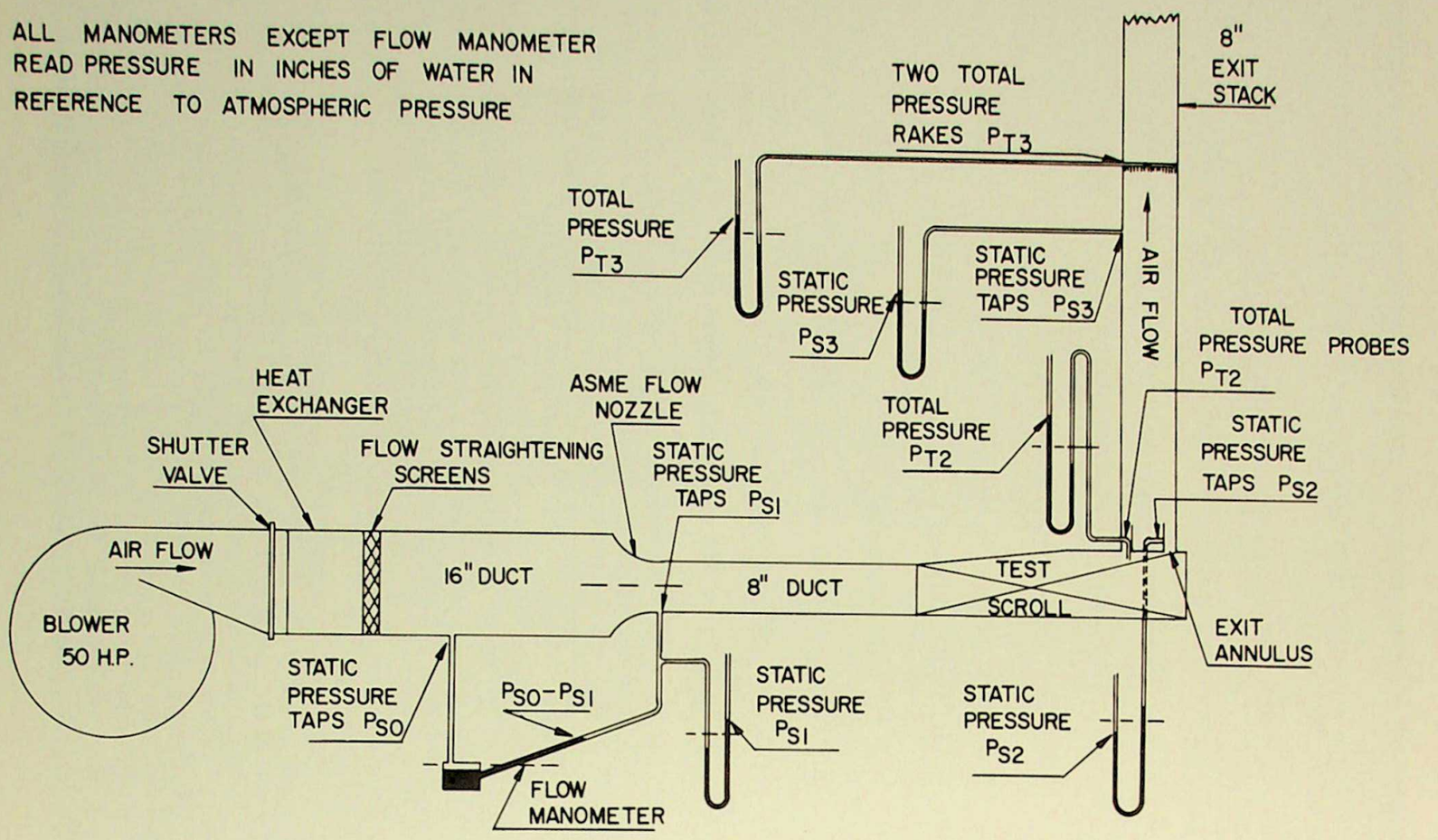

PWAC - 300
FIG 15

E. TEST PROCEDURE

test procedure used for each series of scroll model tests differed in specific details and therefore, described in the following two general categories.

RS-7 Model Scroll Tests

The initial step, after mounting the test scroll into the stand, was to attach and align the instrumented inner and outer cylindrical rings which form the downstream portion of the scroll exit annulus. These rings were also indexed circumferentially relative to the central scroll body and could be rotated through an arc of 45 degrees from a zero reference position.

To start the test cycle, the upstream air cooler was placed in operation and the blower was started. The flow rate was first manually adjusted by a butterfly valve in the blower inlet duct and then the fine adjustments were accomplished with a shutter valve in the 16 inch discharge duct. The pressure differential across the flow meter was read on an inclined water manometer.

All scroll modifications were initially tested at a flow rate of 1000 cubic feet per minute. Tests were repeated with the flow rate increased in 500 cubic feet per minute increments up to the maximum obtainable. For each flow rate tested, the instrumented cylinders on the scroll discharge were rotated through increments of ten degrees from the zero reference position. Five positions were recorded for each flow rate setting.

The data recorded at each setting included the flow nozzle differential pressure, the average static pressure at the discharge of the ASME flow nozzle, the 16 total pressure readings at the midstream point in the exit annulus, and the 16 inner wall static pressure readings in the exit annulus. The temperature of the air stream was recorded periodically.

Tangential Scroll Model Tests (RS-11 through RS-15)

After mounting the test scroll in the stand, the instrumented exit adapter rings were installed and the exhaust stack centered over them.

The starting of the test cycle and adjustment of flow rate was accomplished in the same manner as for the RS-7 model tests.

All scrolls were tested at 1000, 1300, 1500 cfm and at the maximum attainable flow rate. For each flow rate tested, the total pressure Kiel probes were aligned to indicate maximum pressure.

After all five scrolls were tested, a turning vane adapter was added before the exit adapter in an attempt to reduce the high exit swirl and produce a more axial flow pattern. Four of the Kiel probes were replaced by yaw probes placed at the leading edge, 1/4, 3/4 and trailing edge positions of four separate blades to indicate the angle at which the air left the turning vanes. The yaw probes were balanced manually by connecting a U-tube manometer to the balance lines. The data recorded at each setting included the flow nozzle differential pressure, the average static pressure at the discharge of the ASME flow nozzle, the 20 total pressure readings at the midstream point in the exit annulus, and the 40 inner wall static pressure readings in the exit annulus. Other data recorded at less frequent intervals included the temperature of the air stream, the average total pressure and the average static pressure in the exit stack, and the angle at which the air entered the total pressure probes in the exit annulus when turning vanes were used.

F. RESULTS OF TESTS

The results of the turbine scroll tests are presented in terms of: 1) the head loss coefficient, K, and 2) the circumferential velocity distribution at midstream in the exit annulus preceding the turbine nozzle vane assembly.

1. Head Loss Coefficients

The non-dimensional head loss coefficient, $K = \Delta H/(V^2/2g)$, for each of the scrolls tested appears in Fig 16. The total head loss, ΔH, is equal to the difference between the total head in the inlet duct at the exit of the flowmeter and the average total head in the scroll exit annulus. The velocity, V, is the velocity in the eight inch diameter inlet duct and was determined from the continuity equation. This velocity was used as it was common to all the scrolls tested and allows for direct comparison of the different scrolls. The loss coefficients are presented for the different modifications of the RS-7 model scroll with varying number of support vanes and for different changes within a modification. For the tangential inlet model scrolls, they are given for tests with and without the turning vane assembly. The data reduction equations used are given in the appendix.

2. Circumferential Velocity Distribution

The velocity at a circumferential station in the scroll exit annulus was determined from the difference between the measured total and static pressures at that station. The circumferential velocity distributions for all the RS-7 scroll models, including the original configuration, Modification I, and Modification II, are shown in Fig 17 for a flow of 2000 cfm. These plots represent the distribution with 16 scroll support vanes installed and for the Modification II with an inlet section area ratio of 0.85. The loss coefficient for each plot is indicated beside the graph. The velocity distribution is shown for a flow rate of 2000 cfm and the flow patterns were of the same general shape for all the other flows tested. The velocity distribution in the exit annulus for the tangential inlet model scrolls, RS-11 through RS-15, is shown in Fig 18 for a flow of 1300 cfm with and without the turning vane assembly. The maximum percent deviation of the exit velocity from the mean value as determined from the velocity distribution plots for all the model scroll tests is shown in Fig 16.

FIG 16

TABLE OF HEAD LOSS COEFFICIENTS AND VELOCITY DISTRIBUTION FOR ALL MODELS TESTED

$K = \frac{\Delta H}{V^2/2g}$

	-Flow-						Midstream Velocity at Specified Flow			
	1000 cfm	1300 cfm	1500 cfm	2000 cfm	2500 cfm	3000 cfm	Average Velocity FPS at Flow		Deviations in Percent	
RS7 Original										
16 Scroll Support Vanes	6.52		6.97	7.46	7.82		132	2000	+142	-187
8 Scroll Support Vanes	4.82		5.12	5.60	5.92		151	2000	+109	-81
4 Scroll Support Vanes	4.25		4.42	4.49	4.57	4.65	156	2000	+95	-81
0 Scroll Support Vanes	4.52		4.69	4.78	4.88		148	2000	+108	-78
16* SS Vanes & Nozzle	5.52		6.00	6.04			148	2000	+116	-206
RS7-Mod I										
16* SS Vanes	5.38		5.74	5.80		6.28	136	2000	+111	-37
8* SS Vanes	5.30		5.66	5.64		6.11	145	2000	+90	-85
4* SS Vanes	5.19		5.62	5.74		6.10	146	2000	+23	-37
16* SS Vanes & Nozzle	5.34		5.62	5.72			142	2000	+86	-45
RS7-Mod II										
16* SS Vanes	1.47			1.71		1.75	145	2000	+41	-25
16* SS Vanes & Nozzle	1.55		1.33	1.29			143	2000	+24	-16
16** SSV, Nozzle & Dowels	2.78			2.14		2.12	105	2000	+69	-159
16** SSV, Nozzle & Dowels Covered	9.92		9.74				109	1500	+39	-81
16** SSV, Dowels Covered:										
Area Ratios: 1.26				2.16			142	2000	+58	-42
1.07				2.12			142	2000	+32	-34
0.85				2.28			144	2000	+30	-32
0.65				2.92			143	2000	+57	-35
0.51				4.47			142	2000	+32	-30
0.43				4.98			145	2000	+67	-37
RS-11										
No Turning Vanes	0.96	0.79	0.47				191	1300	+5	-5
Turning Vanes	2.27	2.71	2.12				137	1300	+12	-12
RS-12										
No Turning Vanes	0.33	0.42	0.32				132	1300	+4	-3
Turning Vanes	1.21	1.35	1.43				137	1300	+5	-7
RS-13										
No Turning Vanes	1.48	1.20	0.37				179	1300	+7	-9
Turning Vanes	2.88	2.55	2.46				136	1300	+15	-19
RS-14										
No Turning Vanes	4.13	4.81					213	1300	+4	-4
Turning Vanes	6.40	6.10	6.43				145	1300	+14	-14
RS-15										
No Turning Vanes	0.83	0.86					175	1300	+10	-8
Turning Vanes	1.79	1.91	1.68				132	1300	+15	-26

*SS - Scroll Support
**SSV - Scroll Support Vanes

FIG 17

CIRCUMFERENTIAL VELOCITY DISTRIBUTION FOR ALL MODIFICATIONS OF THE MODEL RS-7 SCROLL

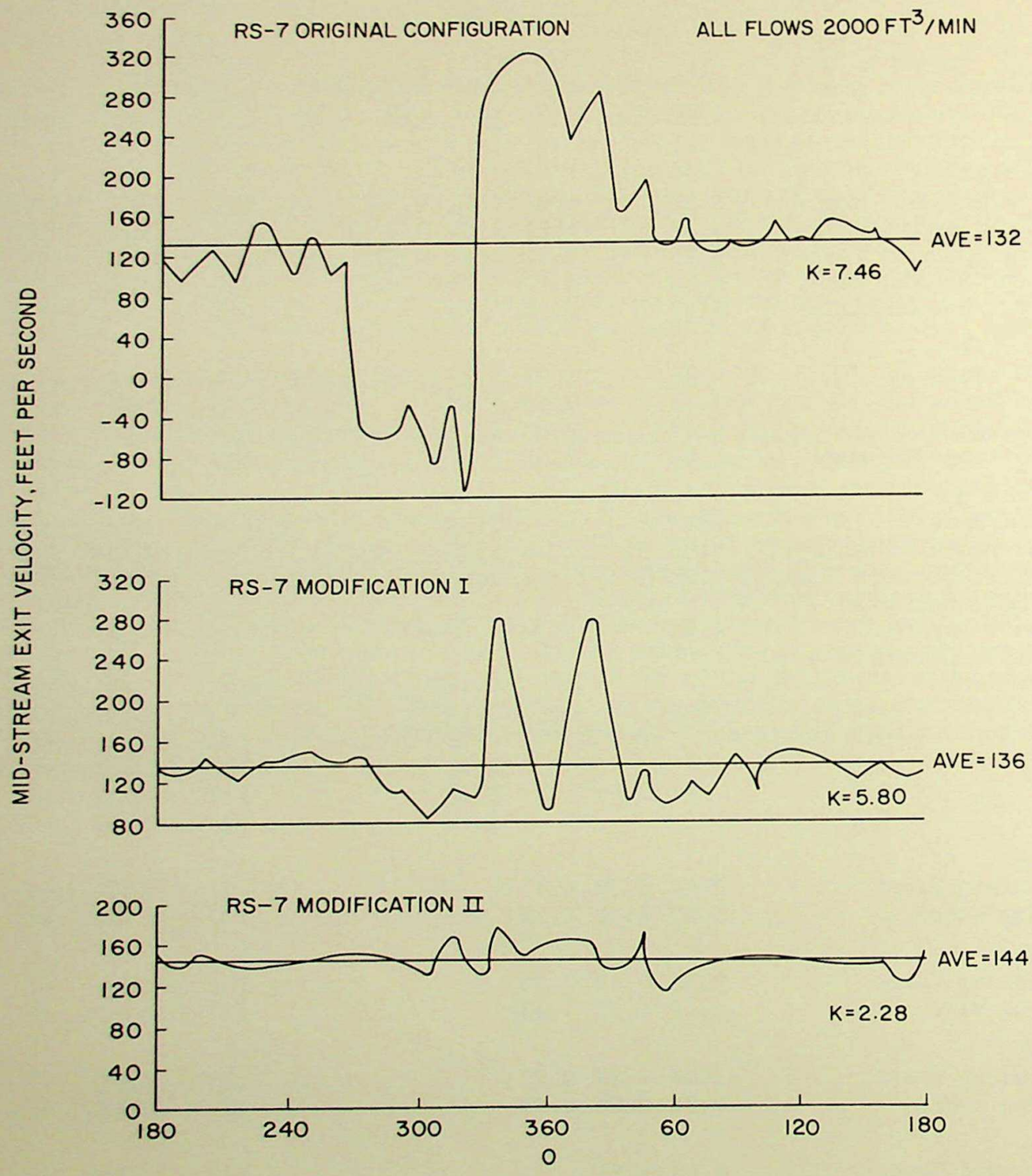

FIG 18

CIRCUMFERENTIAL VELOCITY DISTRIBUTION FOR THE TANGENTIAL INLET MODEL SCROLLS

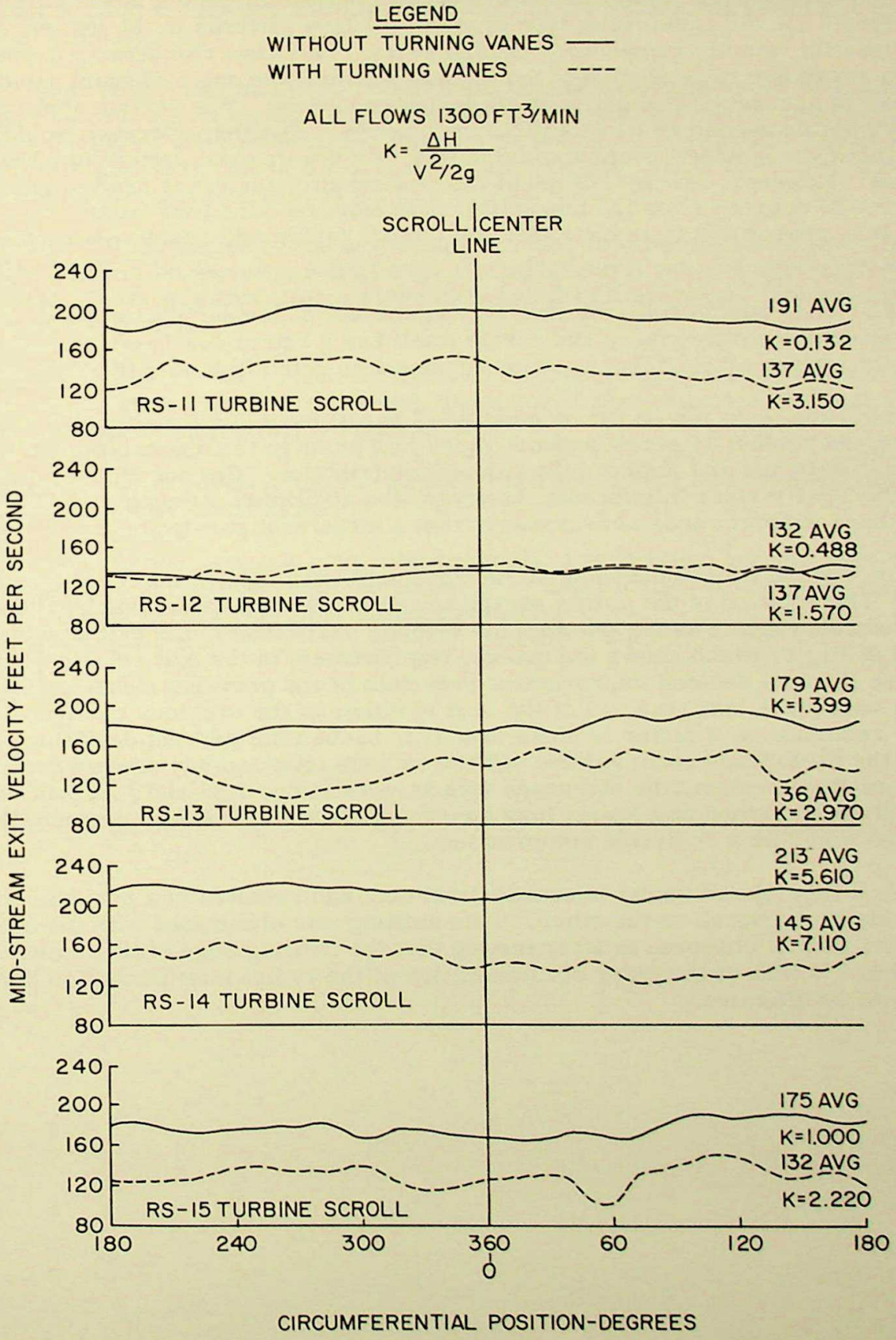

G. DISCUSSION OF RESULTS

Although the loss factors shown for the tangential inlet scrolls are in some cases less than those indicated for the radial inlet type scrolls, the flow patterns in the exit annulus contained highly tangential velocity components or high swirl. This flow characteristic could possibly be used to advantage in the design of the turbine nozzle if the angle of swirl could be predicted with sufficient accuracy, especially at off design conditions. For certain applications, the nozzle may not be needed at all with this type of scroll. Another approach would be the addition of turning vanes which would direct the flow to a nearly axial pattern upstream of the turbine nozzle. However, as can be seen in the test results, the vanes used to turn the flow axially to about 30 degrees from the tangential plane increased the loss factory by a substantial amount. It is reasonable to assume that any further turn would result in a further loss of total pressure.

In using the radial inlet scroll, the flow leaving the scroll is nearly axial which matches the inlet of the turbine nozzle ring. The nozzle itself has a rather low loss characteristic and provides accurate control of the direction of the accelerated flow onto the turbine rotor blades.

The results of the tests run on the original RS-7 scroll model indicated that it was possible, by reducing the number of scroll support vanes just prior to the discharge annulus, to both reduce the loss factor and improve the velocity distribution. For the high temperature application of the TP-1 turbine inlet scroll, however, the additional strength afforded by retaining all of these support vanes is necessary from a structural standpoint.

Modification I of the RS-7 model was an improvement over the original configuration on the 16 vane test. The addition of the nozzle served to reduce the loss factor slightly for the same number of scroll support vanes and also the velocity variations in the exit annulus. This is illustrated in Fig 17 which shows the marked improvement in the exit velocity distribution. Modification II was a decided improvement over both of the previous models. The loss factor with all 16 vanes was less than 1/3 of the loss in either of the previous configurations. There was also a reduction by a factor of more than 1/2, in the total percent deviation of the velocities from the mean midstream values. Of the various inlet support devices tested for use in the inlet transition section, the two vanes with area ratios of 0.85 and 1.07 had the most uniform velocity distribution and lowest loss factor, respectively. It was decided that an area ratio of 0.90 would be a desirable compromise.

Early tests on this type of radial inlet transition duct had resulted in a periodic shifting of flow from one side of the scroll to the other. This shifting was eliminated with the use of an inlet flow splitter. It was observed in later testing that the trailing edge of this splitter must extend to within 1/4 inch of the plane of intersection of the radial inlet transition duct with the scroll body to be effective.

H. CONCLUSIONS

œe conclusions derived from these aerodynamic tests of the various turbine inlet scroll ɔıdels are the following:

The scroll loss coefficient and the discharge velocity distribution in the exit annulus for the RS-7 model scroll were highly dependent on the scroll inlet ducting configuration. Changes in the scroll inlet reduced the loss coefficient from 7.46 to 2.12 and reduced the circumferential variation of the exit midstream velocity about the mean value from approximately $\pm$ 150 percent to $\pm$ 30 percent at 2000 cfm.

The reduction of the number of the scroll support vanes in the RS-7 model reduced the loss coefficient and improved the discharge circumferential velocity distribution. However, the additional strength afforded by retaining all of these vanes is necessary from a structural standpoint.

The loss coefficients for the tangential inlet scroll models are generally somewhat lower than those of the radial inlet scroll model, but the exit flow patterns contained highly tangential flow components indicating high swirl.

Of the tangential inlet scrolls, the RS-12 model has the lowest loss coefficient and the most uniform velocity distribution.

As a result of this test program, the inlet to the TP-1 turbopump turbine inlet scroll was redesigned to correspond with the model RS-7 Modification II type inlet with an area ratio of 0.90 between the inlet splitter vanes.

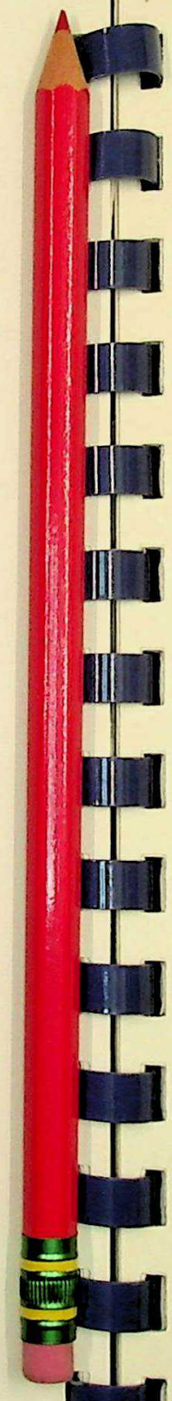

IV. STRUCTURAL TESTS OF THE PROTOTYPE TURBINE INLET SCROLL

A. BACKGROUND AND PURPOSE

In order to insure structural integrity of a component, some knowledge of the stresses and strains in the component at operating conditions is essential. Since analytical techniques for a complex structure are not usually adequate, and direct measurements of strain or stress are not feasible at the operating temperatures involved, a majority of the information sought must come from extrapolation of experimental results obtained at room temperature.

On this basis, room temperature elastic Stresscoat and Strain gage tests were initiated on the TP-1 Turbine Scroll. To simplify test procedures further, static pressure loading was substituted for the hydrodynamic loading encountered during operation.

B. DESCRIPTION OF PROTOTYPE TEST SCROLL

The turbine scroll tested was the stainless steel prototype version of the RS-7 model described in the previous section under scroll aerodynamic development. It is shown in cross section in Fig 3 and set up on the scroll stress test stand in Fig 19. The turbine scroll was fitted with a sealing ring in the exit annulus and a sealing plate on the outlet to permit pressurization.

C. TEST EQUIPMENT AND INSTRUMENTATION

Hydrostatic pressure was used to pressurize the test unit. The pressure was regulated by an air pressure regulator operating through a water accumulator, the pressure being read on a zero to 300 psi gage. A schematic of the test setup is shown in Fig 20.

Strain gage rosettes were applied to the scroll where possible at points of maximum strain as determined from the Stresscoat tests. Rosettes were fabricated from Baldwin FAP - 12 - 12 and FAP - 25 - 12 foil gages. These gages have gage lengths of 0.125 and 0.250 inch, respectively. The smaller gages were used in areas where steep stress gradients were found. Measurements were made during strain gage tests with a Baldwin SR-4 Indicator-Type N.

FIG 19

PROTOTYPE STAINLESS STEEL TP-1 TURBINE AIR INLET SCROLL ON THE HYDROSTATIC STRUCTURAL TEST STAND

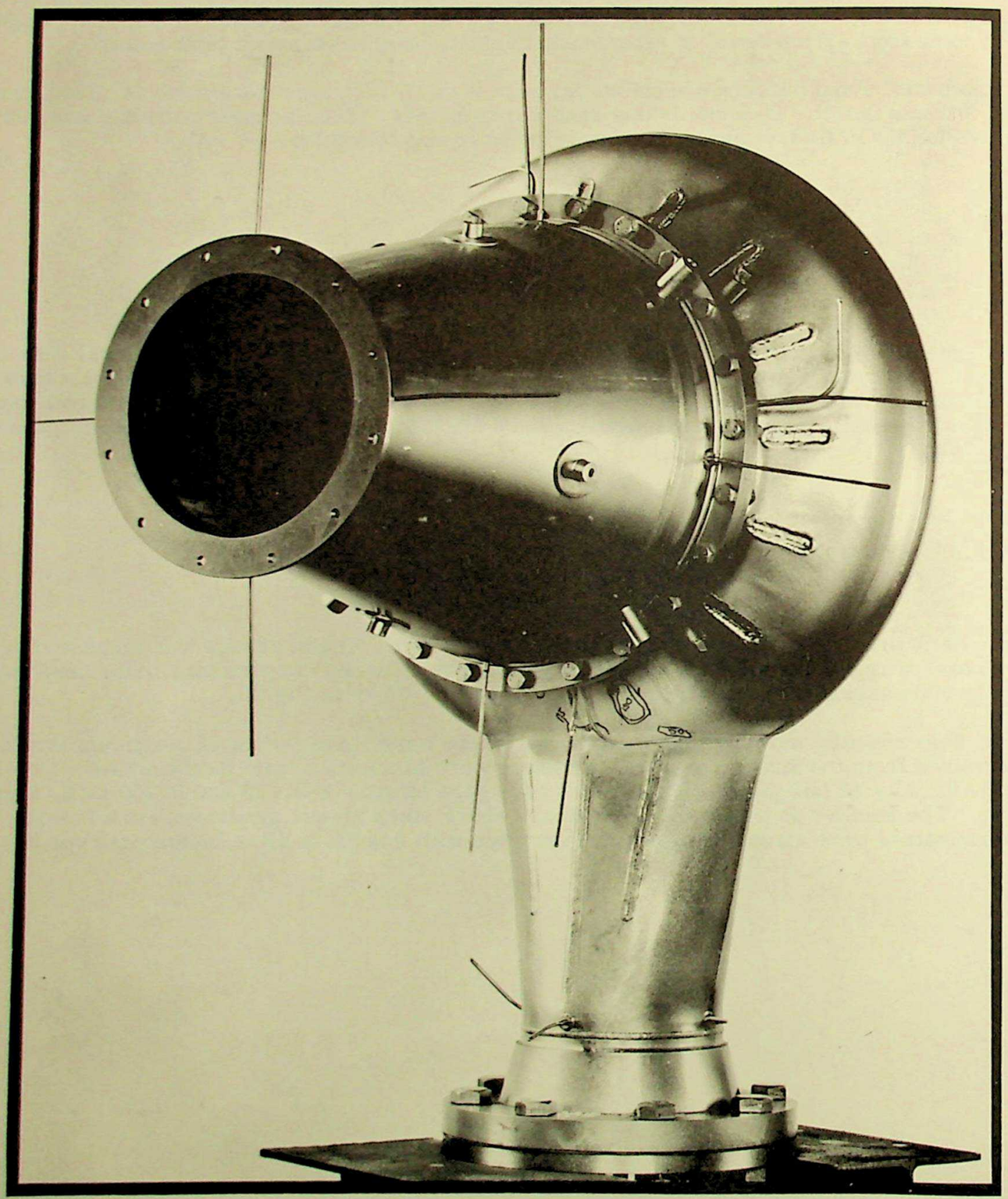

FIG 20

TP-1 AIR INLET SCROLL PRESSURE CONTROL SCHEMATIC

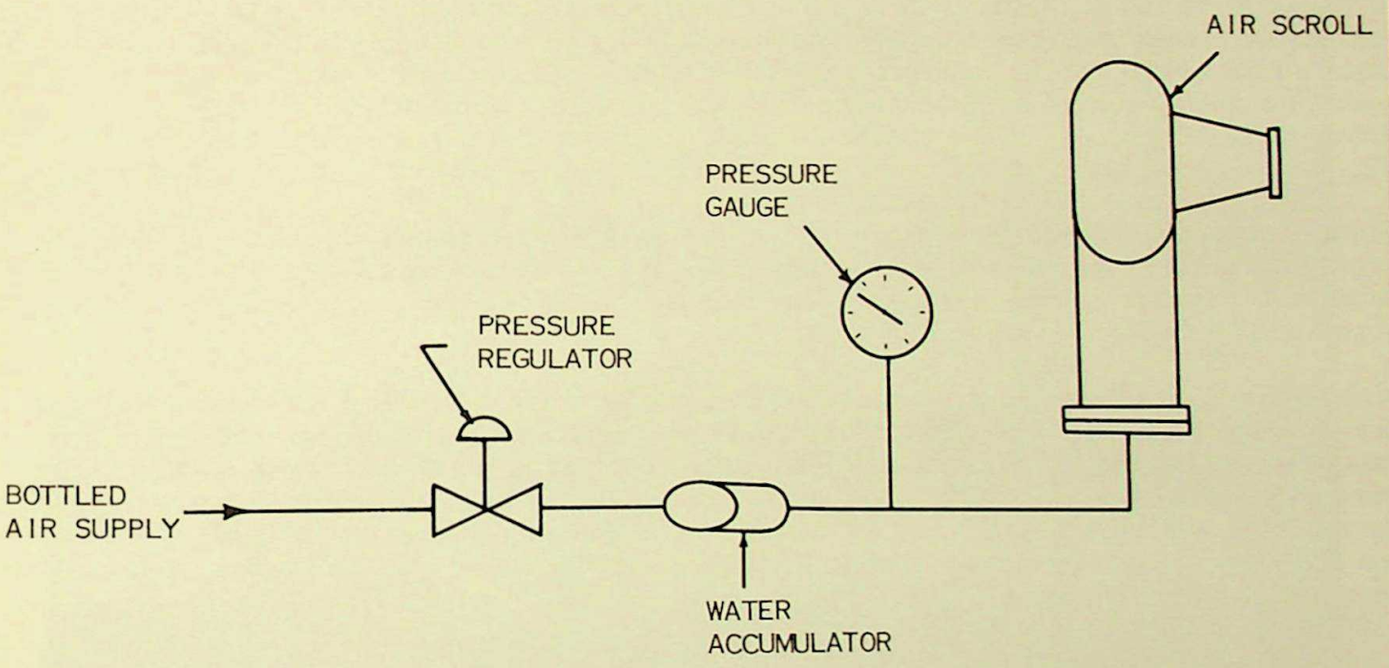

D. TEST PROCEDURE

Three Stresscoat tests were run on the scroll using established Stresscoat procedure. Two were run under normal internal pressure. On the third test, the model was pressurized prior to application of the Stresscoat. During the test, the pressure was then decreased and the compressive stress pattern obtained.

E. RESULTS OF TESTS

In the first Stresscoat test, with positive pressure, initial cracks were observed between 100 and 150 psi. The threshold sensitivity of the coating was 825 micro inches per inch. Because of the large increment of pressure taken in the first test, the test was rerun. In this second test initial cracks were observed between 90 and 100 psi, with a threshold sensitivity of 800 micro inches per inch. In both tests, the most highly stressed areas were found to be the weld joining the torus to the inlet section and the tangential weld on the inside of the torus. Photographs of the model, showing the over-all crack pattern, are presented in Figs 21 and 22. These photographs were taken at a maximum pressure of 175 psi during the first test.

Initial cracks were observed in the reversed pressure test, between 85 and 90 psi effective pressure, at the scroll support vane welds on the inside of the torus. The threshold sensitivity was 650 micro inches per inch. The over-all crack pattern at 175 psi effective pressure appears in photographs in Figs 23 and 24.

Strain gage data were taken at pressures of 50, 100, and 150 psi. The location of the rosettes are shown in Figs 23 and 24. Since the strains were extremely linear, for reduction of the data, stresses at the 100 psi pressure level only were used. Principal strains and stresses were calculated for each rosette. For the latter, values of 28.6×10^6 and 0.3 were used for the modulus of elasticity and Poisson's ratio, respectively. The results of both strain gage and Stresscoat tests are summarized in Fig 25. It will be noted that Stresscoat results have been scaled to a test pressure of 100 psi.

FIG 21

STRESSCOAT CRACK PATTERN AT 175 POSITIVE PRESSURE IN THE VICINITY OF THE INLET DUCT

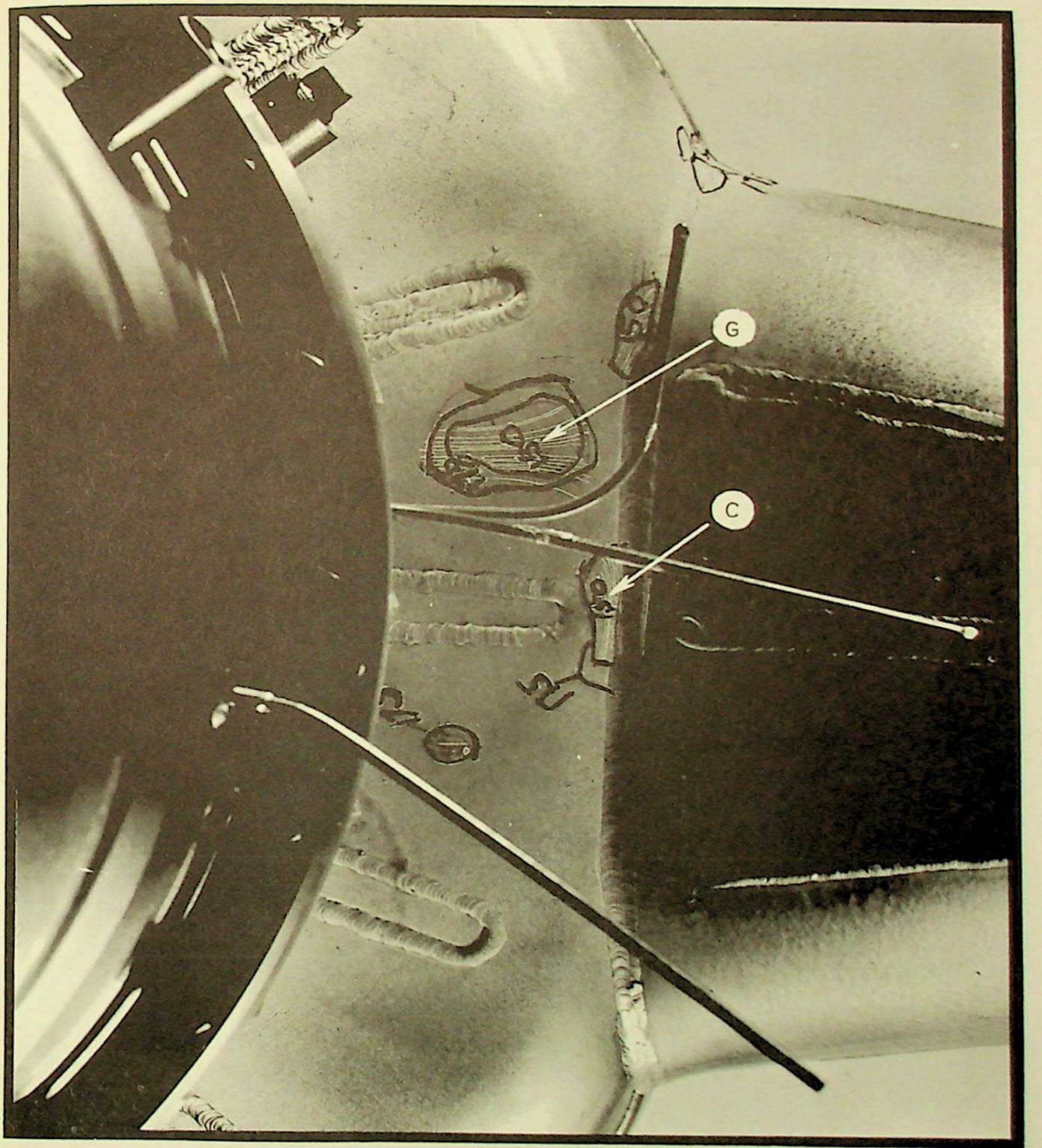

INITIAL CRACKS ARE NOTED AT 150 PSI
THRESHOLD SENSITIVITY - 825 MICROINCHES/INCH
O→ POSITION OF SUBSEQUENTLY APPLIED STRAIN GAGE ROSETTE

FIG 22

STRESSCOAT CRACK PATTERN AT 175 PSI POSITIVE PRESSURE ALONG CIRCUMFERENTIAL WELD

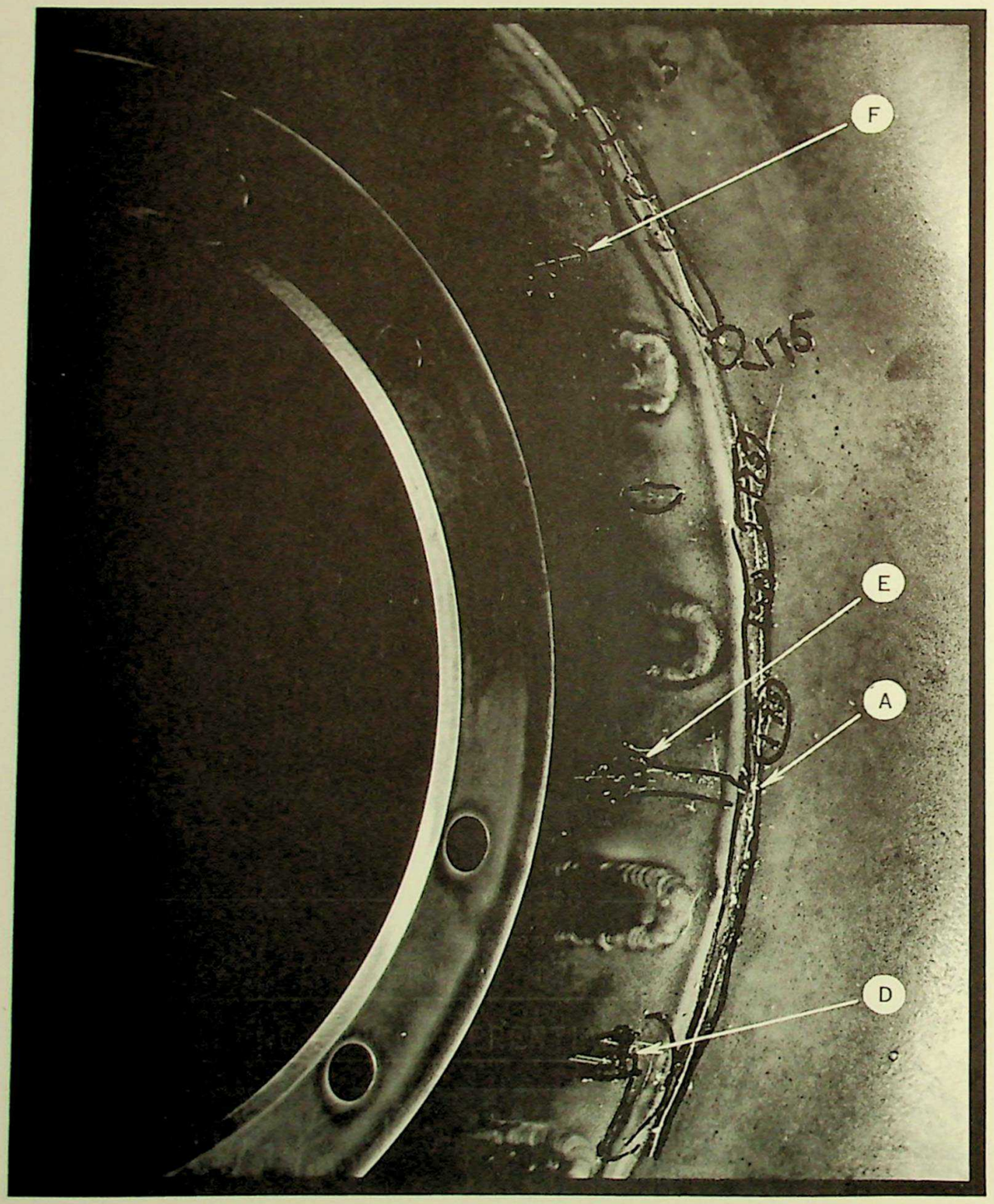

INITIAL CRACKS ARE NOTED AT 150 PSI
THRESHOLD SENSITIVITY - 825 MICROINCHES/INCH
O ⟶ POSITION OF SUBSEQUENTLY APPLIED STRAIN GAGE ROSETTE

FIG 23

STRESSCOAT CRACK PATTERN AT 175 PSI NEGATIVE PRESSURE IN THE VICINITY OF THE OUTER RADIUS OF THE WELDS

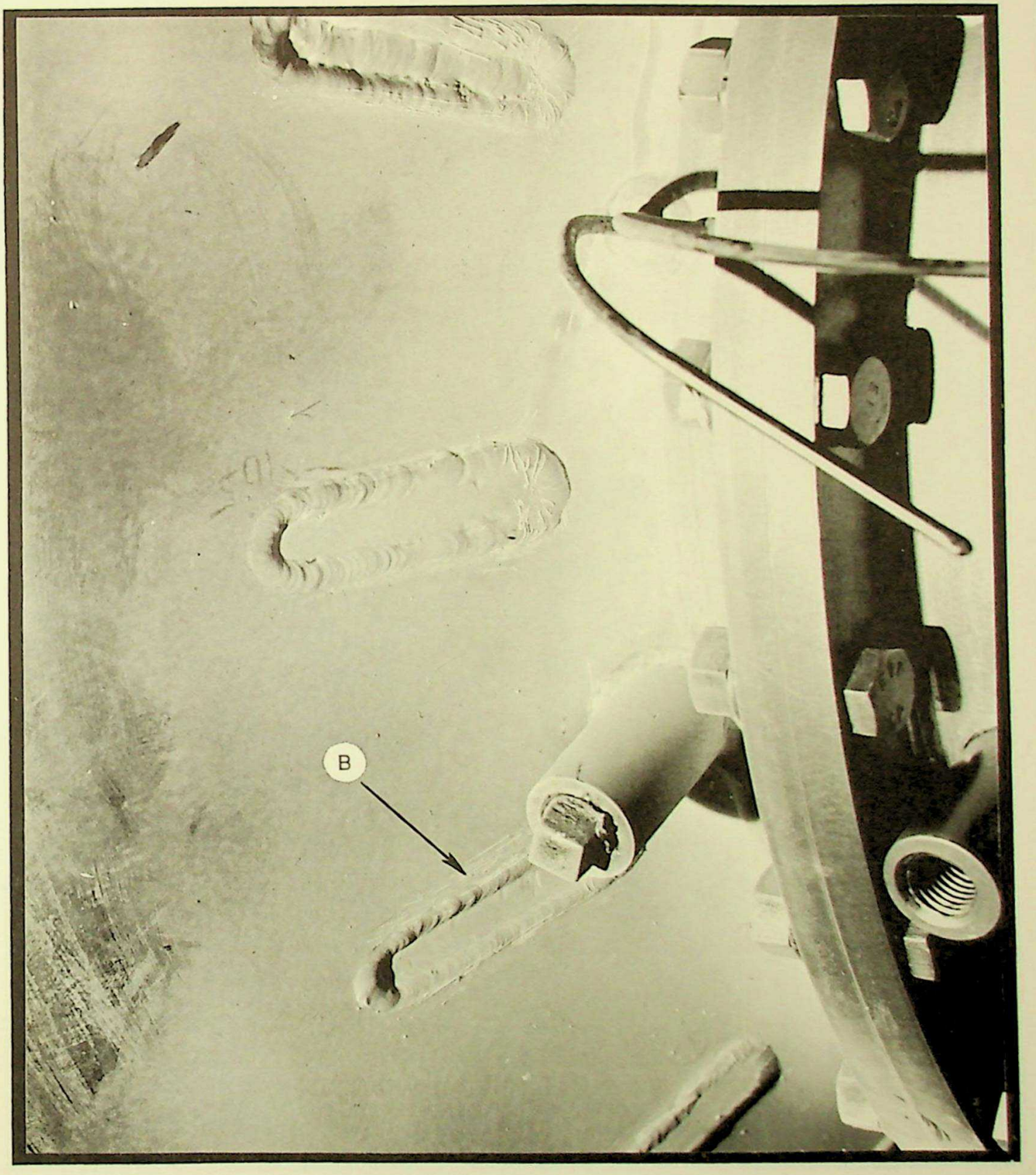

INITIAL CRACKS APPEARED AT 105 PSI
THRESHOLD SENSITIVITY - 650 MICROINCHES/INCH
○ ⟶ POSITION OF SUBSEQUENTLY APPLIED STRAIN GAGE ROSETTE

FIG 24

STRESSCOAT CRACK PATTERN AT 175 PSI NEGATIVE PRESSURE AT THE INNER RADIUS OF THE VANE WELDS

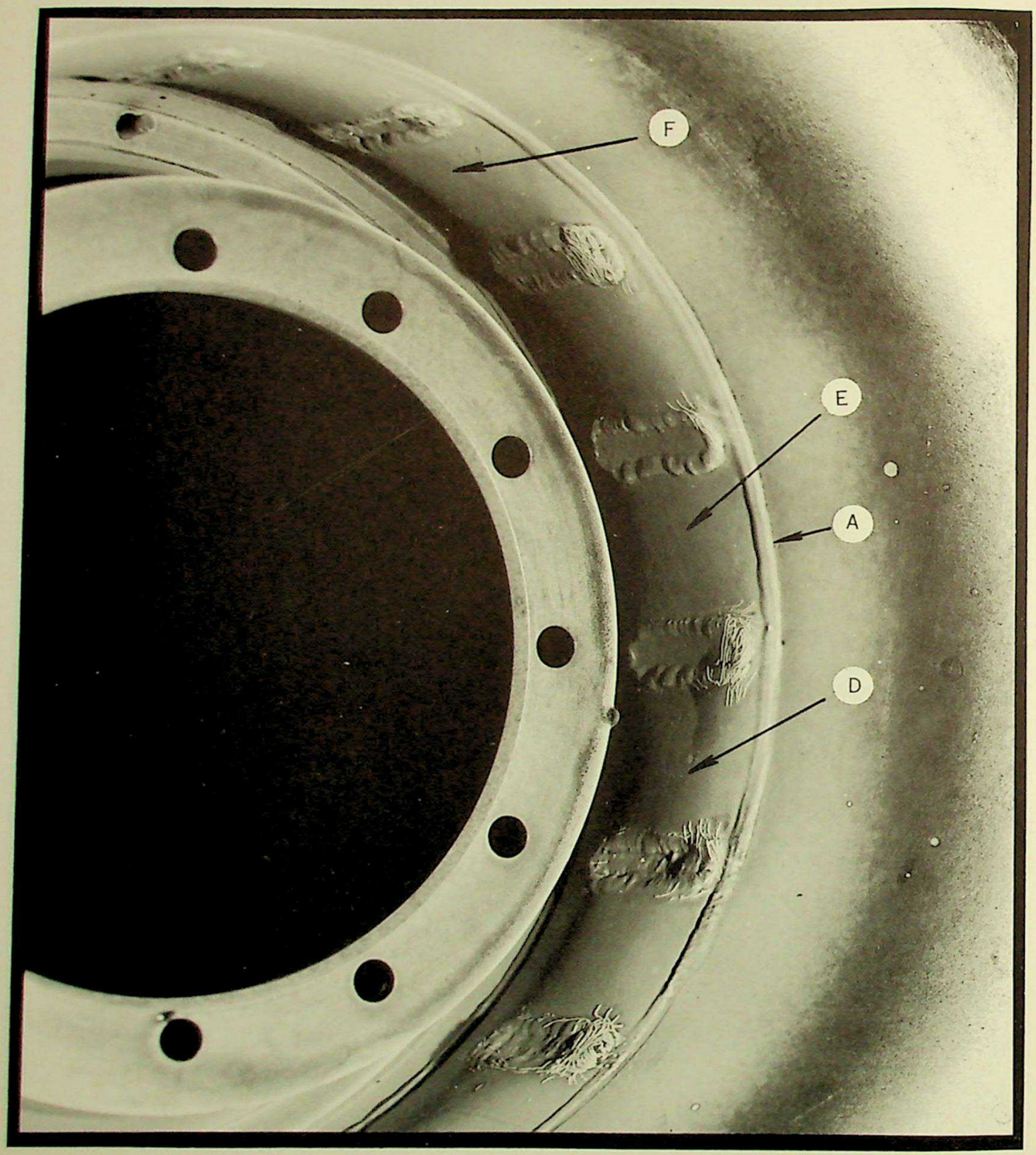

INITIAL CRACKS APPEARED AT 95 PSI
THRESHOLD SENSITIVITY - 650 MICROINCHES/INCH

TABLE OF HYDROSTATIC STRESS TEST RESULTS OF THE TP-1 TURBINE INLET SCROLL

Area	Rosette	Max Strain At 100 psi (Stresscoat) μ in/in	Max Strain At 100 psi (Strain Gages) μ in/in	Max Stress (Est.) At 100 psi (Stresscoat) psi	Max Stress At 100 psi (Strain Gages) psi	Max Stress At Design Pressure - 35 psi psi
Weld on inside of torus	(2) A	840	555	27,200	18,000	9,500
Vane weld root on outside of torus	(2) B	-650	-431	-19,000	-12,600	6,700
Weld at junction of torus with inlet pipe	(2) C	840	579	27,000	18,600	9,500
Between vane roots on inside of torus	(3) D	550	372	17,900	12,100	6,300
Between vane roots on inside of torus	(3) E	550	527	17,800	17,100	6,200
Between vane roots on inside of torus	(3) F	490	431	16,300	14,300	5,700
Between vane roots on outside of torus	(3) G	640	599	20,800	19,400	7,300
(1) Vane weldments on inside of torus	-	-720	-	-20,600	-	-7,200
(1) Root of instrumentation boss	-	790	-	22,400	-	7,800

(1) Insufficient area to mount strain gages

(2) FAP-12-12 gages

(3) FAP-25-12 gages

F. DISCUSSION OF RESULTS

Correlation of results obtained by the two types of tests is reasonable in areas where no sharp stress gradients exist. Where these gradients appear, however, Stresscoat data show considerably higher strain values than those obtained by strain gages. Two effects contribute to this difference. In general, the steep gradients were found to exist on or near welds. Since a strain gage cannot be applied to the uneven weld surface, it was necessary to apply the gage a small distance away from the most highly stressed areas. Secondly, the strain gage measures not peak strain, but average strain over its gage length.

In evaluating the stresses in the scroll, therefore, data obtained by Stresscoat should be of prime consideration. To account for biaxiality, however, reference to the strain gage results must be made. On this basis an estimated maximum stress is obtained from Stresscoat data by multiplying the maximum stress determined by strain gages by the maximum strain determined by Stresscoat and dividing this product by the maximum strain determined by strain gages.

Scaling the results of the tests to a design pressure of 35 psi, maximum stresses of 9, 500 psi were found, located on the torus to inlet section weld and the inside tangential weld of the torus. A summary of the stresses at design pressure appears in Fig 25.

Since strains were obtained on the outside of the collector only, bending and membrance components cannot be separated by use of test data. Analysis of the scroll body showed membrane stresses of 700 and 300 psi to exist in the torus in the meridional and circumferential directions, respectively. Subtracting the 700 psi component from the maximum total stress of 9, 500 psi observed, the bending component of stress at these areas can be estimated to be 8, 800 psi. Because they are induced by discontinuties of the scroll geometry, these bending stresses will tend to relieve themselves during high temperature operation. Since the tensile strength of type 316 stainless steel is 34, 000 psi at 1425F the possibility of short time failure of the turbine scroll under the influence of the discontinuity stresses is negligible.

V. TURBINE FACE SEAL DEVELOPMENT

A. BACKGROUND AND PURPOSE

The turbine seal in the TP-1 turbopump was designed to control the leakage of the oil and oil vapor from the bearing compartment into the hot airstream. The design consists of a carbon face seal in series with a labyrinth as shown in Fig 26. Cool air is supplied to the cavity between the seal and labyrinth to maintain a pressure which is 4 psi lower than that existing in the bearing compartment. This flow also helps to cool the face seal in addition to lowering the pressure differential across it. Face seal proposals from numerous commercial companies were studied and designs from Sealol Corporation, Cartriseal Corporation, and Chicago Rawhide Manufacturing Company were selected for evaluation. The following tests were conducted on the face seal only under simulated prototype operating conditions. The last test was extended to provide information on the endurance life of the face seal.

B. DESCRIPTION OF TEST FACE SEALS

Schematics of the face seals installed in the test unit are shown in Fig 27. Three seals were fabricated with carbon faces running against stainless steel mating rings and used rubber "o" rings for the secondary seal. The Chicago Rawhide and Cartriseal units were loaded with wave springs while the Sealol design used a series of coil springs for loading. The different methods used to mount the mating rings were: the Chicago Rawhide ring was clamped directly against stainless steel shoulder without any secondary sealing; the Cartriseal ring was held against a soft copper gasket by a wave spring; the Sealol ring was held in position by a spirolox washer with a pin to prevent rotation and a rubber "o" ring for the secondary seal. Photographs of the three face seals tested are shown in Figs 28, 29, and 30.

C. DESCRIPTION OF TEST EQUIPMENT AND INSTRUMENTATION

This test program was conducted in two identical test stands; one of which is shown in Fig 31. These stands were powered by 5 hp, 2000 to 10,000 rpm, Varidrive motors. The mating rings were mounted directly on the output shaft of the Varidrives and the face seals mounted in a vessel bolted to the Varidrive housing. Cooling oil was supplied to the seal from a 2 gpm oil system with manual flow control and automatic temperature control. Pressures on both sides of the test seal were controlled separately by 125 psig non-bleeding regulators and read on 50 psi Heise gages with dial graduations in 0.1 psi increments and $\pm$ 0.1 percent accuracy. The regulators were supplied with air during all but the final test which used argon. The oil leakage was collected and measured by the instrument shown in Fig 32. The gas leakage was measured by either a 200 cc/min or 2000 cc/min rotometer with an accuracy of $\pm$ 2 percent. Temperatures were indicated on a 24 point Brown Precision Indicator with a range of 0 to 2000F and a $\pm$ 1 percent accuracy. The power input to the drive motor was recorded on a 5 kw Esterline Angus Wattmeter which was accurate to 0.05 kw.

SCHEMATIC OF TURBINE FACE SEAL AND LABYRINTH

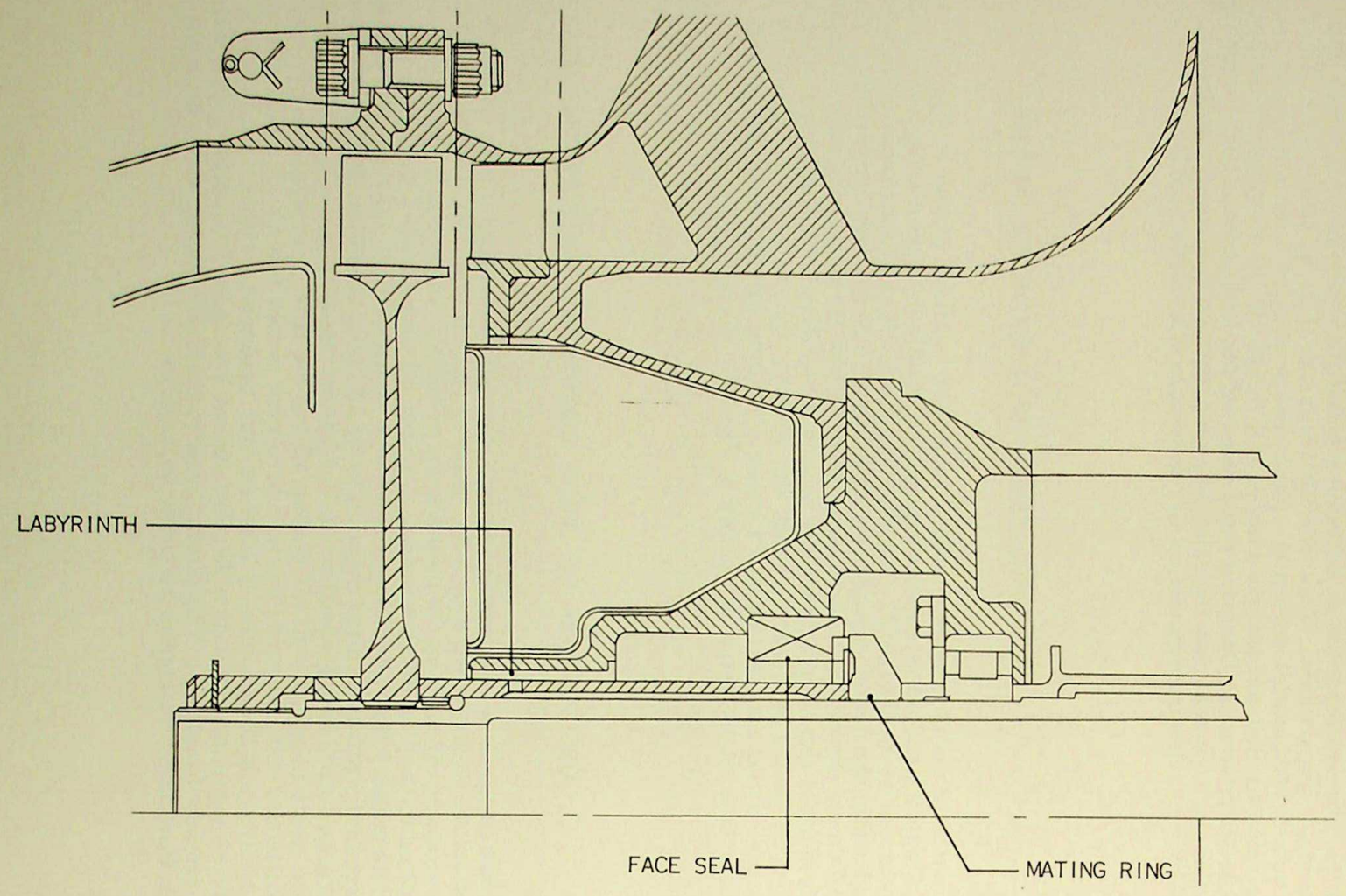

PWAC - 300
FIG 26

FIG 27

TEST RIG INSTALLATION SCHEMATICS OF COMMERCIAL TURBINE FACE SEALS

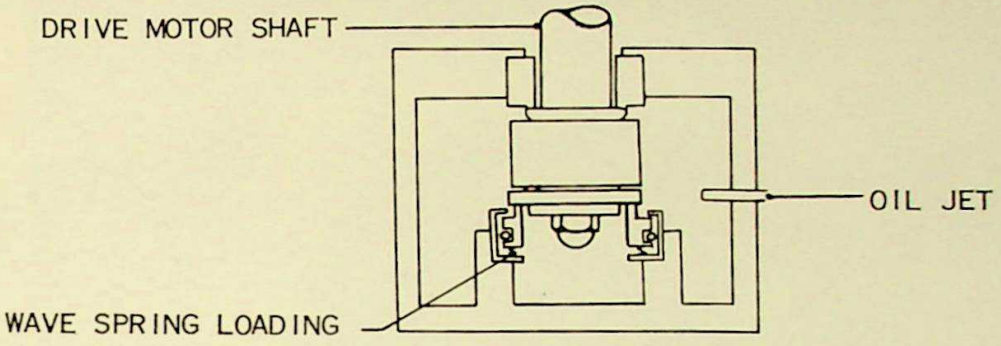

CHICAGO RAWHIDE CARBON FACE O RING SEAL

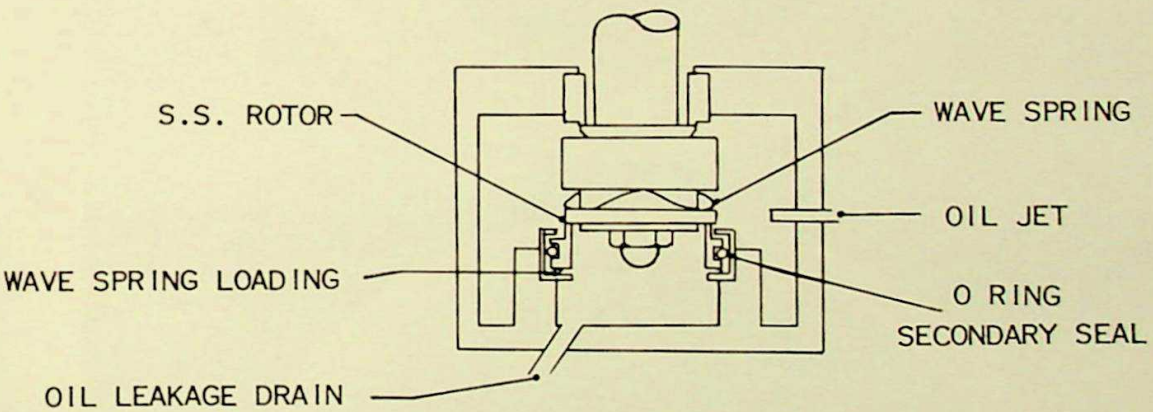

CARTRISEAL CARBON FACE O RING SEAL

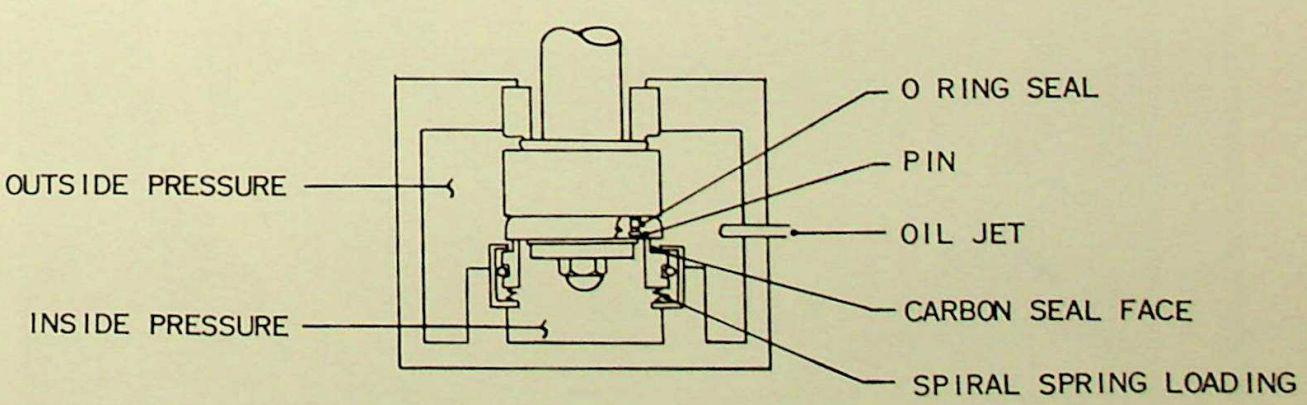

SEALOL CARBON FACE O RING SEAL

FIG 28

8D6163

SEALOL FACE SEAL AFTER 208 HOURS TESTING

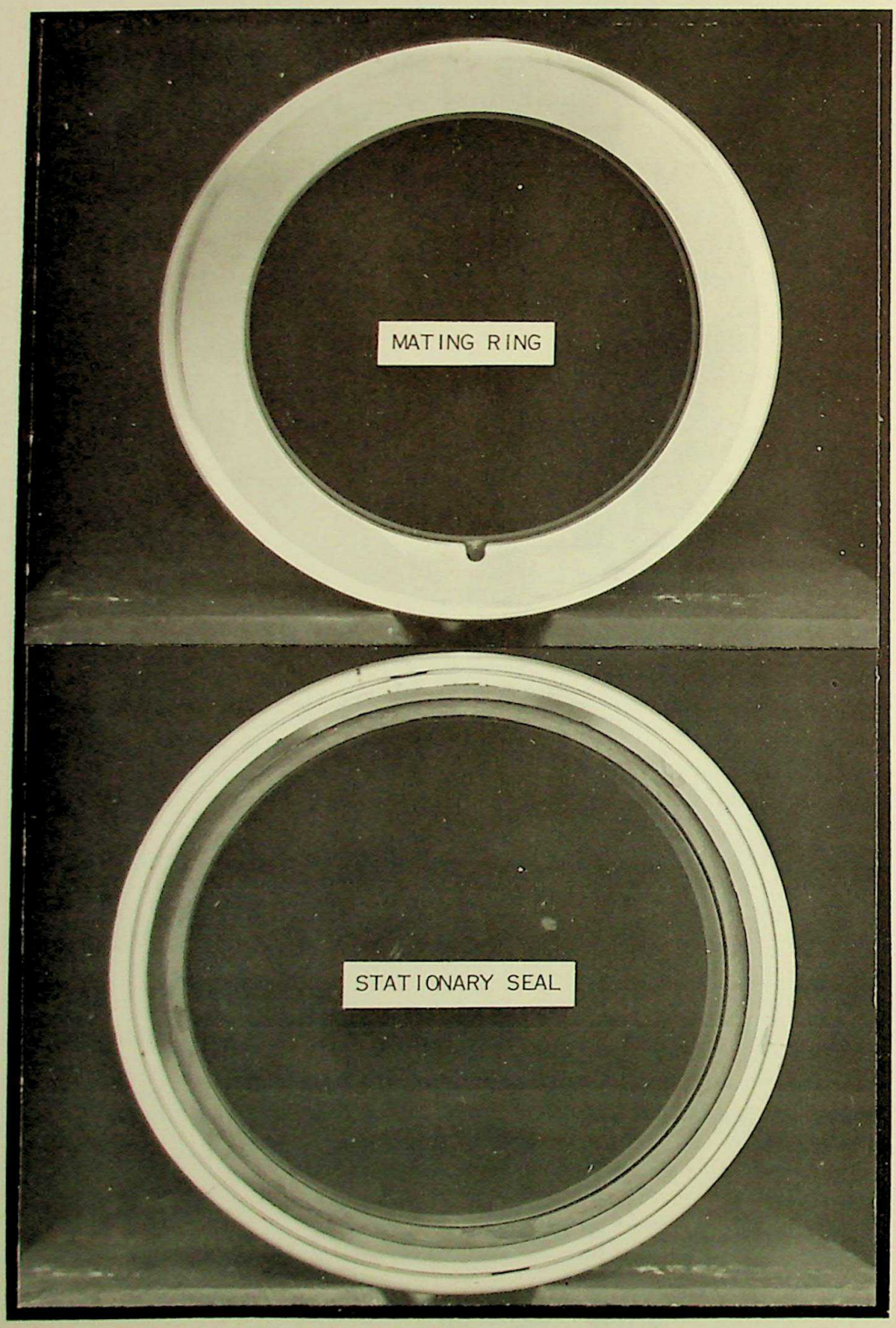

FIG 29

8D5596

CHICAGO RAWHIDE SEAL AFTER 34 HOURS OF TESTING

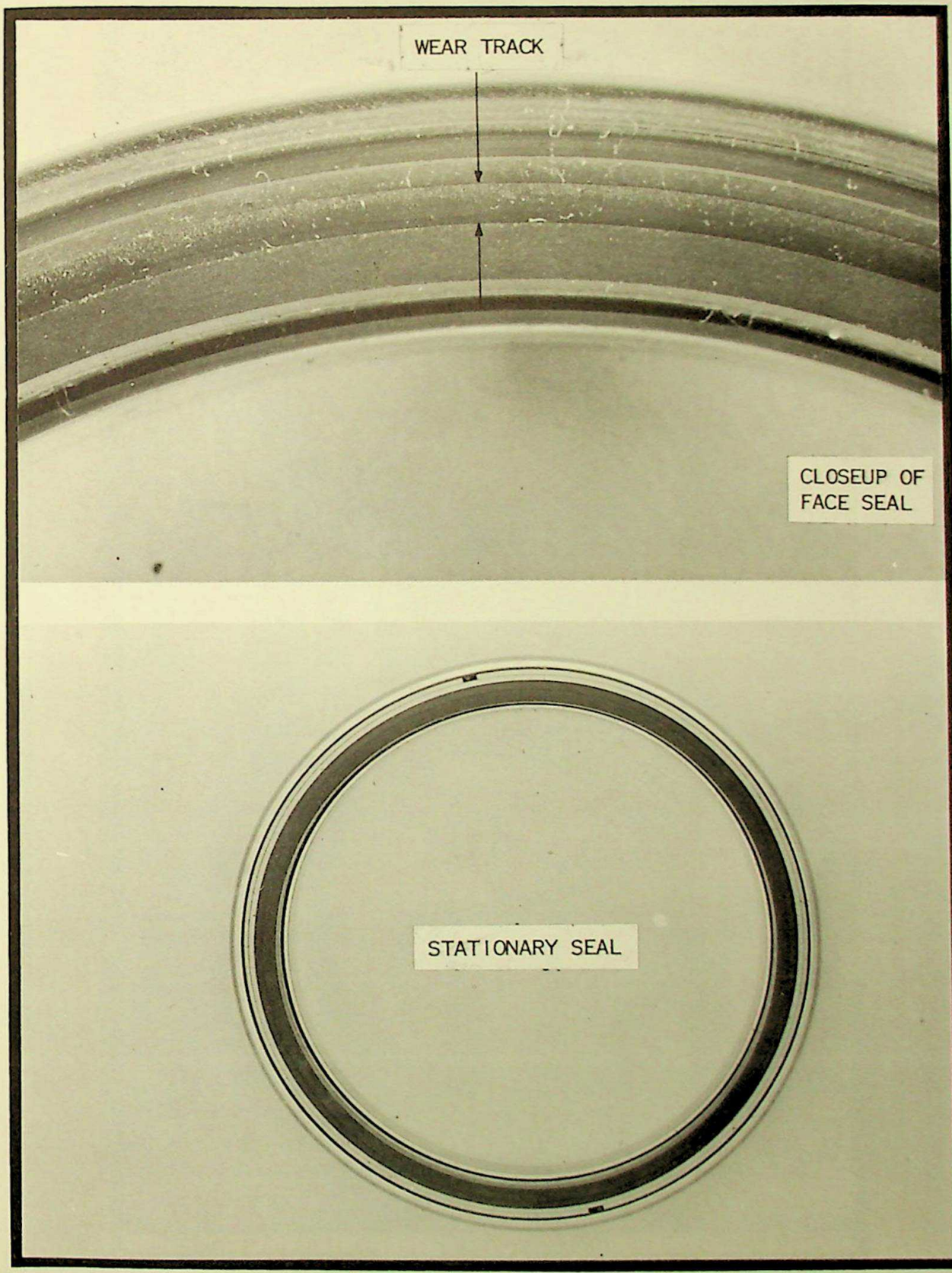

FIG. 30

8D5813

CARTRISEAL SEAL AFTER 282 HOURS OF TESTING

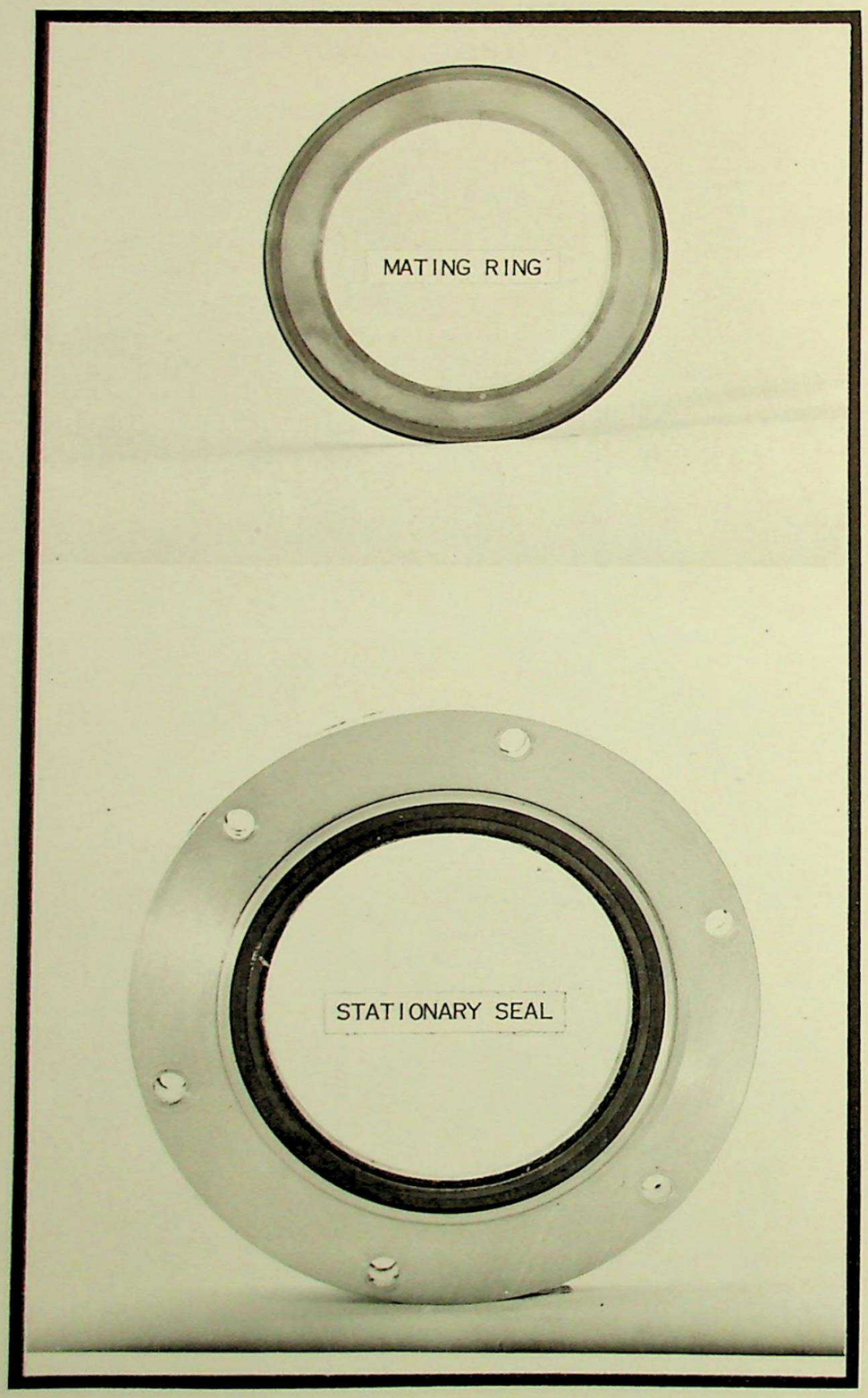

FIG 31

8D6509 8D6510

TEST STAND USED FOR TURBINE FACE SEAL EVALUATION

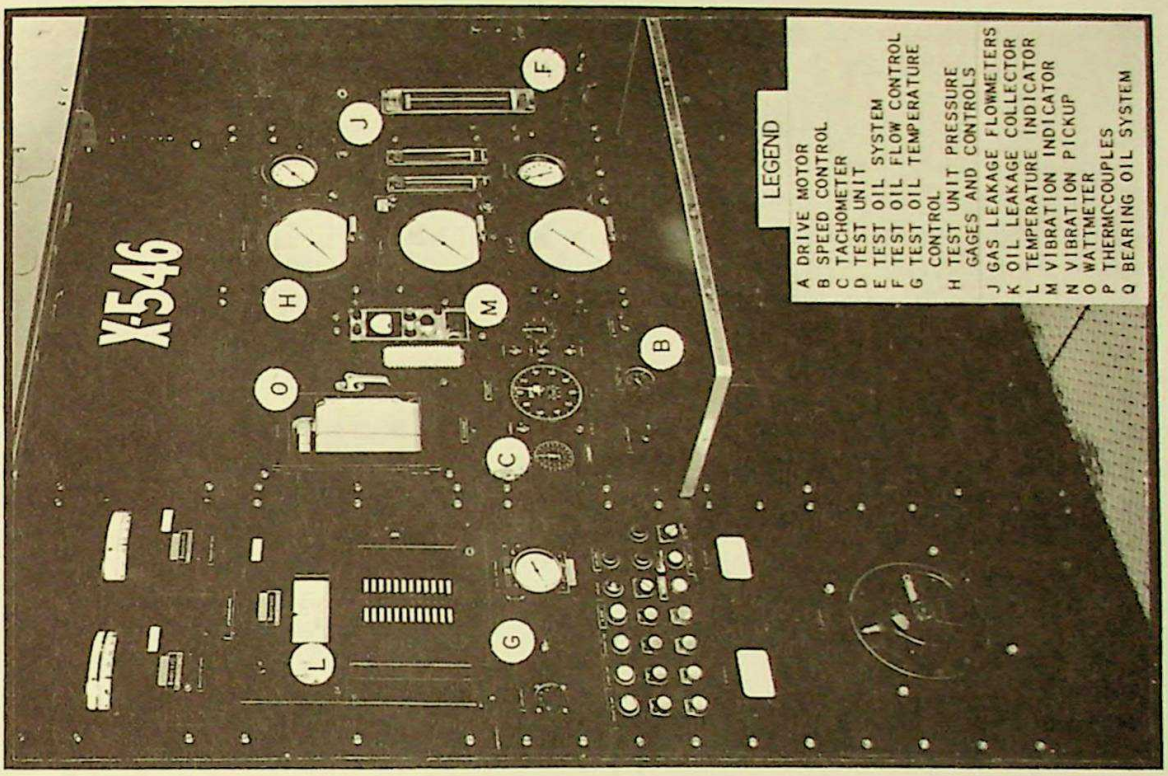

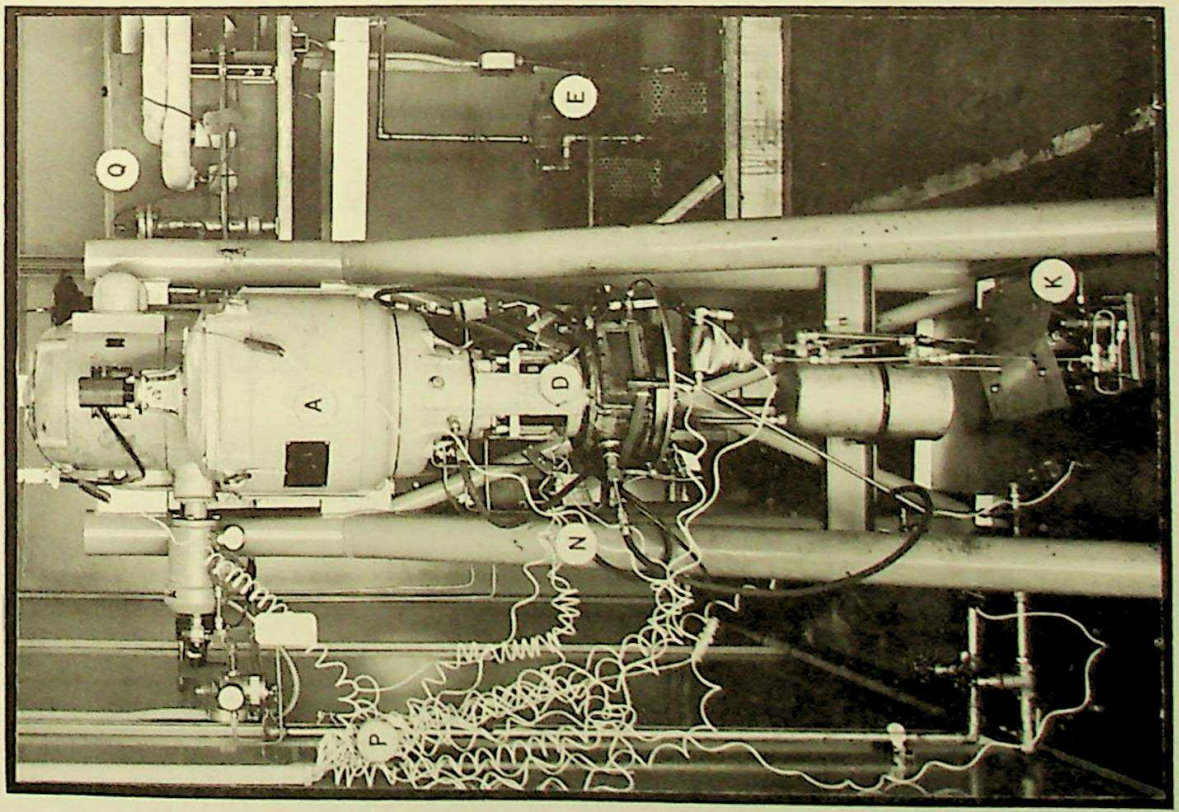

FIG 32

SCHEMATIC OF OIL LEAKAGE MEASURING DEVICE

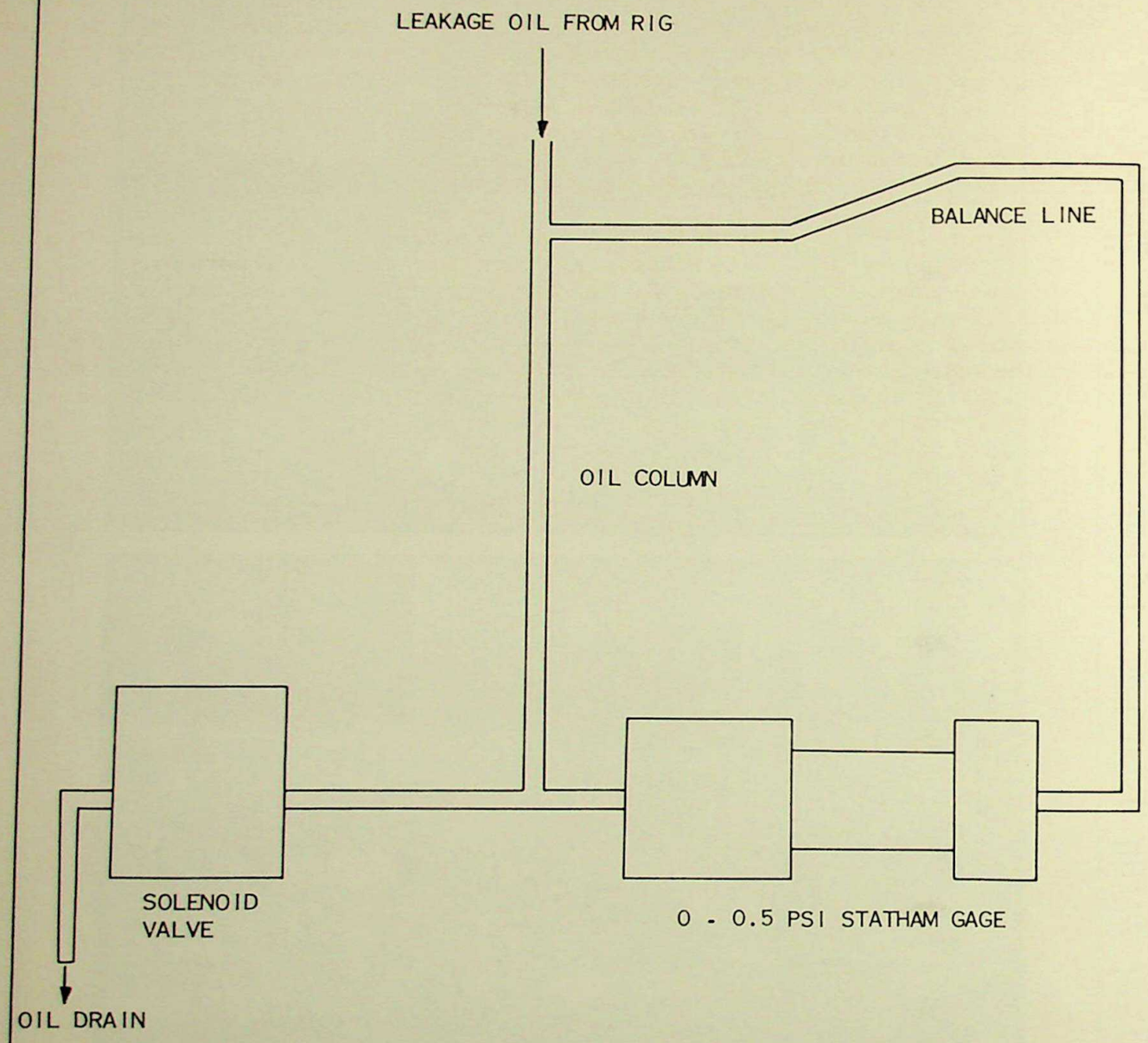

THE PRESSURE EXERTED BY THE COLUMN OF LEAKAGE OIL IS MEASURED BY THE STATHAM GAGE AND TRANSMITTED AS A MILLIVOLT SIGNAL. THE EFFECT OF GAS PRESSURE IS NULLIFIED BY THE BALANCE LINE. WHEN NECESSARY THE LEAKAGE OIL MAY BE DRAINED BY OPENING THE SOLENOID VALVE. LEAKAGES AS SMALL AS 1/50 OF A C.C. MAY BE DETECTED.

D. TEST PROCEDURE

The mating rings were installed into the test rig with less than 0.001 inch radial and axial runouts. It was found that this yielded the best seal results and also eliminated the necessity of rebalancing the mating ring or the rotating assembly. It was also found necessary to lap the faces of the seal to closer tolerances than as supplied. A standard of four micro inches rms surface finish and a flatness of one-half helium light band was established in the latter part of this seal program. The seals were tested at speeds of 3000, 6000, and 8000 rpm. At times these test speeds were altered by as much as 1000 rpm to eliminate undesirable vibrations due to stand limitations. Cooling oil was injected on the rotating seal from one radial oil jet flowing 0.2 to 0.6 gpm of grade 1010 mineral oil, MIL-0-6081A, with a 25 psi differential through the jet nozzle. In later tests, MIL-L-7808 oil replaced the MIL-0-6081A oil to reduce the high temperature breakdown of the oil. The oil inlet temperature was automatically controlled at 120F $\pm$ 5F and both inlet and discharge temperatures were recorded hourly.

The face seals were tested for 50 to 100 hour intervals at several intermediate speeds between 2000 and 8000 rpm and for at least 100 hours at 8000 rpm to determine the performance characteristics of the particular seal design. Testing was discontinued when leakage was excessive and showed no signs of decreasing. The last test, No. 12, was conducted for almost 1400 hours to gain information regarding the endurance life of the seal. For this test, thermocouples were installed on the stationary seal to determine the approximate face seal running temperature at the rubbing faces. After testing, the rotating seal was again checked for radial and axial runout. Both stationary and rotating seals were then photographed and inspected for surface finish, flatness, and depth and width of wear track.

E. DISCUSSION OF RESULTS

The results of the seal tests in this program are summarized in tabular form in Fig 33. For the cases where the tests were cut short because of excessive leakage, wear measurements were not made. For the most part, the power consumption and wear were reasonable low. Figs 28, 29, and 30 show typical seals after testing with no visible signs of deterioration.

Oil leakage, which varied from 0.17 to 130 cc/hr, was a principal factor by which to ascertain the success or failure of each seal test. In this respect, the Chicago Rawhide seal was the most decisive failure. This seal was also the most simple and conventional design. The most probable causes of this failure were either an out of parallel condition of the installed mating ring mounting surfaces or improper loading or "hang up" of the stationary seal. The mounting surfaces of the mating rings supplied by the vendor were found to be 0.0007 inch out of parallel whereas the vendor recommended less than 0.0004 inch.

The Cartriseal seal yielded the most satisfactory and consistent results of the three types tested. This was true even though the mating ring stackup was the most complicated. In all tests on this seal, the leakage was below 0.5 cc/hr. There was no loss in performance of this seal during the endurance test, No. 12, and at the time of completion of the test the seal appeared to be in perfect operating condition.

The Sealol face seal was found to be erratic in the leakage rates between individual seal tests which ranged from 1.6 to 30 cc/hr. This could be at least partially attributed to the rather complicated mating ring assembly and also to the "o" ring secondary seal. It was found that the secondary seal which Sealol Corp. supplied with its face seal units swells in the presence of MIL-0-6801A oil. This could result in "hang up" of the seal face. Difficulty was also found in obtaining and maintaining the runouts on the mating ring due to the spirolox washer stackup.

It was found that oil leakage may be minimized by: lapping the seals to a flat, fine finish; using secondary "o" ring seals that are compatible with the oil being used; using an oil that does not breakdown at the highest operating temperature; and installing the face seal with sufficient care to maintain critical runout limits.

TABULATED SUMMARY OF THE TP-1 TURBINE FACE SEAL TEST RESULTS

Test No.	Seal Manufacturer	Test Conditions: Speed Range rpm	Oil Flow gpm	Type of Oil	Type of Gas	Pressure, psig Inside	Pressure, psig Outside	Seal Performance: Oil Leakage cc/hr	Power Consumption kw	Seal Temperature, F	Wear, inches Rotating	Wear, inches Stationary	Time, hrs/Speed, rpm	Total Test Time	Remarks
1	Cartriseal	6000	0.33	MIL-0-6081A	Air	0	4	0.17	0.6	--	0.00002	--	154/6000	154	Test complete
2	Chicago Rawhide	3000 6000	0.60	MIL-0-6081A	Air	0	4	130	0.1	--	--	--	6/6000	23	High leakage failure
3	Sealol	3000 to 8000	0.60	MIL-0-6801A	Air	0	4	2.5	0.5	--	0.00003	0.00001	258/8000	333	Test complete
4	Chicago Rawhide	3000 to 6000	0.60	MIL-0-6801A	Air	0	4	18	0.4	--	0.035	--	60/6000	119	High leakage failure
5	Cartriseal	3000 to 9000	0.33	MIL-0-6801A	Air	0	4	0.4	0.4	--	0.00015	0.007	109/9000	276	Test complete
6	Chicago Rawhide	3000	0.33	MIL-0-6801A	Air	0	4	25	0.1	--	--	--	51/3000	51	High leakage failure
7	Sealol	3000 to 9000	0.33	MIL-0-6801A	Air	0	4	10	0.5	--	--	--	50/9000	194	High leakage failure
8	Sealol	3000 to 8000	0.33	MIL-0-6801A	Air	0	4	1.6	0.6	--	0.00004	0.004	118/8000	193	Test completed
9	Sealol	3000	0.33	MIL-L-7808	Argon	0	4	3.5	0.7	--	--	--	5/3000	5	High leakage failure
10	Sealol	3000 to 8000	0.33	MIL-L-7808	Argon	0	4	6	1.4	--	--	--	23/8000	89	High leakage failure
11	Sealol	4500 to 8000	0.22	MIL-L-7808	Argon	0	4	30	0.4	--	--	--	7/8000	17	High leakage failure
12	Cartriseal	3000 to 8000	0.22	MIL-L-7808	Argon	0	4	0.5	0.6	135 to 194	--	0.0265	1291/8000	1391	Test completed

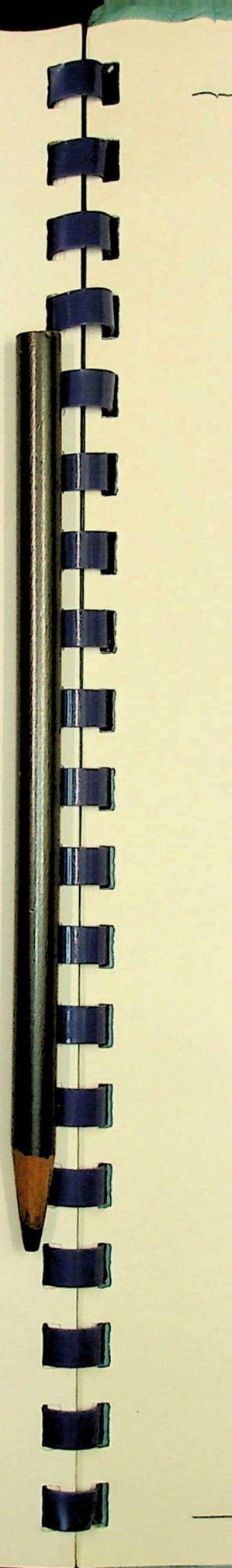

VI. APPENDIX

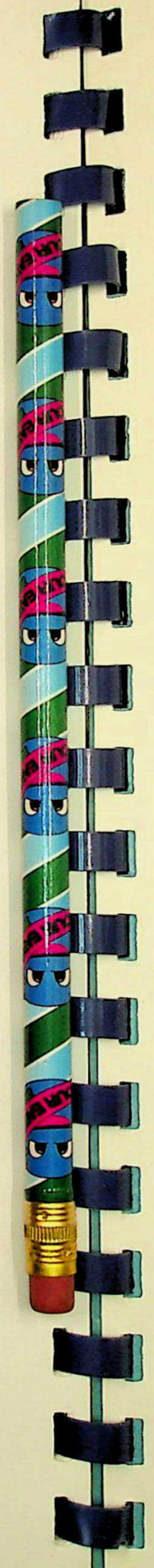

APPENDIX A

DATA REDUCTION EQUATIONS

1. Conversion Constant for Velocity of Air in Feet Per Second to Equivalent Velocity Pressure in Inches of Water

The basic relationship is given as:

$$P_V = \frac{1}{2} \rho V^2 \tag{1}$$

where

ρ is the density of air at standard conditions of 59F and 14.7 psi pressure and is equal to 0.002378 slugs per cubic foot.

Equation (1) thus becomes:

$$P_V = \frac{1}{2} \times 0.002378 \left(\frac{\text{slug}}{\text{ft}^3}\right) \times V^2 \left(\frac{\text{ft}^2}{\text{sec}^2}\right) \tag{2}$$

Correcting equations (2) to obtain P_V in terms of inches of water is done by applying the following conversions:

$$1 \text{ slug} = \frac{1 \text{ lb sec}^2}{\text{ft}}$$

$$1 \text{ ft}^2 = 144 \text{ in.}^2$$

$$27.69 \text{ in } H_2O = 1 \text{ psi}$$

Equation (2) then becomes:

$$P_V = \frac{1}{2} \times 0.002378 \left(\frac{\text{slug}}{\text{ft}^3}\right) \times V^2 \left(\frac{\text{ft}^2}{\text{sec}^2}\right) \left(\frac{\text{lb sec}^2}{\text{slug ft}}\right) \left(\frac{\text{ft}^2}{144 \text{ in.}^2}\right) \times 27.69 \left(\frac{\text{in } H_2O}{\text{psi}}\right)$$

which reduces to:

$$P_V = 0.000229 V^2 \text{ or } V = \sqrt{\frac{P_V}{0.000229}} \tag{3}$$

where

P_V is expressed in inches of water and V is expressed in feet per second.

2. Determination of Total Pressure, P_T, at Flow Nozzle Discharge (Station One)

The Bernoulli equation may be written:

$$P_{T1} = P_{S1} + P_{V1} \tag{4}$$

where

all pressure are expressed in inches of water and psi is the manifolded average of three static pressure taps located at station one and P_{V1} is determined using equation (3) with the velocity based on Q/A

where

Q is the established flow in cubic feet per second
A is the area in square feet of the duct at station one.

3. Determination of Head Loss Coefficient

The equation for the head loss coefficient is:

$$K = \frac{\Delta H}{V^2/2g} \tag{5}$$

where

K is the non-dimensional loss coefficient
ΔH is the total head loss in feet of air
V is the axial velocity in feet per second based on continuity in the eight inch supply duct
g is the acceleration due to gravity (32.2 ft/sec^2)

ΔH is determined as follows:

$$H = (P_{T1} - P_{T2}) \frac{\rho \text{ water}}{\rho \text{ air x } 12} \tag{6}$$

where

P_{T1} is determined from equation (4) in Item 2

P_{T2} is the numerical average of all total pressure readings taken at the midpoint of the exit annulus

and

$$\frac{\rho \text{ water}}{\rho \text{ air x } 12} = \frac{1.94 \text{ (slug/ft}^3\text{) x 1 ft}}{0.002378 \text{ (slug/ft}^3\text{) x 12 in.}} = 67.98 \frac{\text{ft}}{\text{in.}}$$

Substituting these values into equation (6) results in

$$\Delta H = (P_{T1} - P_{T2})\,(67.98) \tag{7}$$

where

$(P_{T1} - P_{T2})$ is in inches of water and ΔH is in feet of air.

V is determined as follows:

$$V = \frac{Q}{A} \tag{8}$$

where

Q is the established flow in cubic feet per second
A is the area of the eight inch supply duct.

Determination of the Velocity at Each Point of the Exit Annulus for Use in Plotting Circumferential Velocity Profile

The basic relationship was derived in equation (3) in Item 1 as:

$$V_2 = \sqrt{\frac{P_{V2}}{0.000229}} \tag{9}$$

where

V_2 is now the velocity in feet per second at the midpoint of the exit annulus at a particular circumferential position and P_{V2} is the velocity pressure in inches of water at the same point.

P_{V2} is determined by re-arranging terms in equation (4) and by changing subscripts to denote station two:

$$P_{V2} = P_{T2} - P_{S2}$$

where

all pressures are in inches of water and P_{T2} is the total pressure measured at the midpoint of the exit annulus and P_{S2} is the static pressure measured at the inner wall of the exit annulus.

RECEIVED

1960 AUG 22 AM 11 46

U.S. ATOMIC ENERGY COMM.
OFFICE OF ASSISTANT GENERAL
COUNSEL FOR PATENTS

PRATT & WHITNEY AIRCRAFT
DEPENDABLE ENGINES